Deep-Sea Research I, Vol. 40, No. 7, pp. 1405–1412, 1993.
Printed in Great Britain.

0967-0637/93 $6.00 + 0.00

Identification of the oxic/anoxic interface by isopycnal surfaces in the Black Sea

CEMAL SAYDAM,* SULEYMAN TUGRUL,* OZDEN BASTURK* and TEMEL OGUZ*

(*Received* 20 *March* 1992; *in revised form* 28 *August* 1992; *accepted* 11 *September* 1992)

Abstract—The analysis of hydrochemical data collected in the Black Sea since 1987 shows that the upper boundary of the oxic/anoxic interface zone coincides with the nitrate maximum at the depths of $\sigma_t \approx 15.40 \pm 0.10$ isopycnal surface. Its lower boundary corresponds to the phosphate maximum depth at $\sigma_t \approx 16.20 \pm 0.05$ isopycnal surface, independent of the geographical location and season. In the absence of the continuous pump cast measurement system, and when the oxygen and sulphide concentrations are too low to be measured with sufficient precision within the interface zone, such features of the oxygen–nitrate and H_2S–phosphate correlations at specific density levels provide a direct and practical way to identify the oxic/anoxic interface zone. This, in turn, allows for a more precise and systematic water sampling for studying the complex biogeochemistry of the layer.

INTRODUCTION

THE Black Sea, the largest anoxic basin in the world, possesses various oceanographic features that make it distinctively different from other marine environments. Among those features, formation of a transitional layer between oxic and anoxic layers and its associated biogeochemistry have been of great interest to marine scientists. In this characteristic layer, the redox potential of the water decreases sharply due to oxygen deficiency and the appearance of hydrogen sulphide at its lower boundary. Based on the measurements of trace level oxygen and hydrogen sulphide concentrations by the conventional titrimetric methods, the co-existence of oxic and sulphidic waters (the so-called C-layer) in this redox zone has been debated for many years (GRASSHOFF, 1975; SOROKIN, 1983; MURRAY *et al.*, 1989; CODISPOTI *et al.*, 1991). At micromolar levels, O(10 μM), the measurements of H_2S and oxygen (hereafter referred to as DO) by conventional titrimetric methods suffer from analytical and sampling errors due to the atmospheric contamination, and therefore require very special sampling and analytical techniques (MURRAY *et al.*, 1989; CODISPOTI *et al.*, 1991). The technical difficulties in the standard titrimetric methods have mistakenly led to overestimation of the layer's thickness (CODISPOTI *et al.*, 1991; MILLERO, 1991).

Using the continuous pump cast measurements, which avoids the water samples from the atmospheric contamination, MURRAY *et al.* (1989) and CODISPOTI *et al.* (1991) have recently shown that the oxygenated and sulfidic waters do not overlap and are separated by

*Middle East Technical University, Institute of Marine Sciences, P.O. Box 28, Erdemli 33761, Icel, Turkey.

the so-called the suboxic zone. In this zone, the oxygen and sulphide concentrations do not overlap and have concentrations too low ($\sim<1$–$5\ \mu$M) to be measured accurately by the conventional titrimetric methods. They also suggested the shoaling of the anoxic sulphidic boundary in recent years. However, KEMPE *et al.* (1990) and TUGRUL *et al.* (1992) have expressed a contrary view, noting that comparison of the existing data do not conclusively demonstrate such a trend in the vertical displacement of the sulphidic boundary.

In the absence of continuous profiling system, properly-collected and closely-spaced water sampling are needed to study the biogeochemistry of this transitional layer. The lack of *a priori* knowledge for the specification of the positions of the boundaries of the oxic/anoxic interface, however, leads to serious sampling problems since this interface zone is subject to considerable spatial variability associated with the mesoscale variability of the circulation and the thermohaline structure of the Black Sea (SOROKIN, 1983; BRYANTSEV *et al.*, 1988; OGUZ *et al.*, 1991, 1992, in press; MURRAY *et al.*, 1991; CODISPOTI *et al.*, 1991). In this paper we attempt to show that the boundaries of the transitional layer, where the nutrients (nitrate and phosphate) reveal some special characteristic features, can be defined with a relative confidence by means of the specific isopycnal surfaces (i.e. σ_t values), independent of geographical location and season. In particular, we show that the upper boundary of the suboxic zone is defined by a specific density level at which a significant correlation exists between the maximum nitrate concentrations and trace level DO concentrations. We also show a similar significant correlation between the large phosphate anomalies and trace level hydrogen sulphide concentrations that defines the lower boundary of the suboxic zone. The transitional (redox) zone, where the DO and H_2S concentrations are too low to be determined accurately by conventional methods, can then be identified easily by means of standard *in situ* CTD measurements.

MATERIALS AND METHODS

The hydrochemical data examined for this study were collected during the cruises of the R.V. *Knorr* in June–July 1988 and the R.V. *Bilim* in 1987–1991, covering mainly the Turkish Exclusive Economic Zone (approximately southern half of the sea), and the R.V. *Dm. Mendeleyev* in August 1989 covering the entire basin. During the R.V. *Bilim* and the R.V. *Knorr* cruises, the hydrographic data were collected by using the Sea-Bird Model SBE-9 CTD system. A Soviet made CTD system was used during the R.V. *Dm. Mendeleyev* cruise. Sea water samples were generally collected by Go-Flo Rosette bottles in the R.V. *Bilim* surveys, and by Niskin bottles in the R.V. *Dm. Mendeleyev* cruise. The continuous pumping system (CODISPOTI *et al.*, 1991) was used in the R.V. *Knorr* surveys we discuss here.

Nutrient analyses were carried out using multi-channel autoanalyser systems by all parties. For the determination of DO and H_2S concentrations, the samples collected by the R.V. *Bilim* and R.V. *Dm. Mendeleyev* cruises were analysed by the conventional Winkler and iodimetric titration methods. For the R.V. *Knorr* cruises, the DO and H_2S concentrations were measured by colorimetric techniques.

RESULTS AND DISCUSSION

We first examine the data obtained by the pump cast measurements in the R.V. *Knorr* 1988 cruises (FRIEDERICH *et al.*, 1990). These are the most reliable and precise DO and H_2S

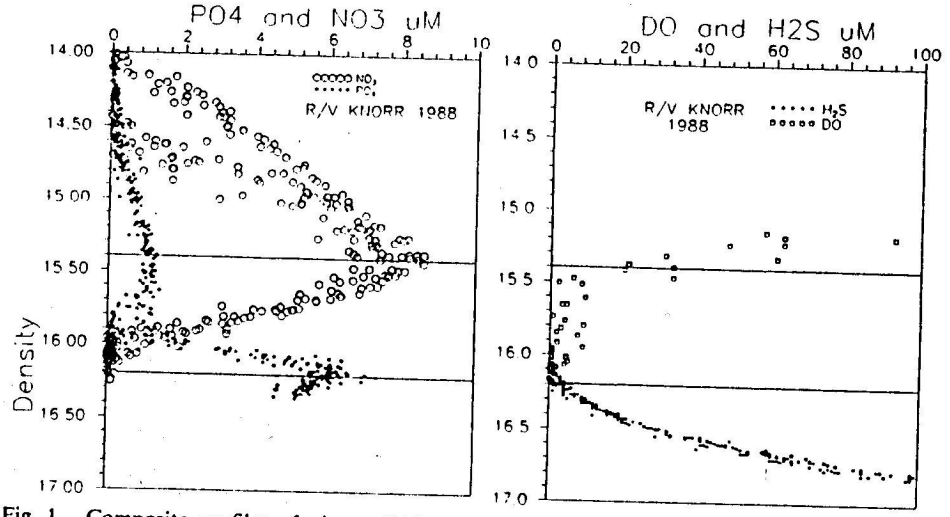

Fig. 1. Composite profiles of nitrate (NO_3), phosphate (PO_4), oxygen (DO) and hydrogen sulphide (H_2S) versus density (σ_t) for 12 pump cast stations of the R.V. *Knorr* 1988 cruises. Density is given in terms of kg m^{-3}, and others by μM.

data, measured accurately up to ~1–5 μM concentrations in the Black Sea. Composite profiles of DO, H_2S, nitrate and phosphate concentrations relative to density (σ_t) at 12 pump cast stations (Fig. 1) reveal that (i) the upper and lower boundaries of the oxic/anoxic interface, defined as the DO <20 μm and H_2S concentrations less than 5 μM, lie between the isopycnal surfaces of $\sigma_t \simeq 15.40 \pm 0.10$ and $\sigma_t \simeq 16.20 \pm 0.05$; and (ii) these density surfaces correspond to the nitrate and phosphate maxima formed at the upper and lower boundaries of this transitional layer, respectively. There is a pronounced increase in the nitrate concentrations starting at the depths corresponding to $\sigma_t \sim 14.0$, and reaching to a maximum of 8–9 μM at the depths of $\sigma_t \simeq 15.40 \pm 0.10$. As stated by MURRAY *et al.* (1989) and MURRAY and IZDAR (1989), the level of this nitrate maximum coincides with the sharp drop in the oxygen concentrations below 20 μM as a result of the denitrification process in the oxygen deficient water (SOROKIN, 1983; SEITZINGER, 1988).

The composite profiles for phosphate exhibits two maxima (SHAFFER, 1986; MURRAY *et al.*, 1989; CODISPOTI *et al.*, 1991). The relatively broad upper maximum, established at the lower boundary of the oxygenated layer, has resulted from the aerobic oxidation of biodegradable organic matter of algal origin and coincides with the nitrate maximum. The deeper maximum has been formed at the upper boundary of the anoxic sulphidic layer. In the relatively narrow density surfaces $\sigma_t = 15.9$ and 16.2, phosphate concentration increases sharply from the minimum levels to the large values to form the deeper characteristic maximum at $\sigma_t = 16.2 \pm 0.05$, significantly correlating with the first appearance of the anoxic sulphidic water, independent of geographical location (see also TUGRUL *et al.*, 1992). SHAFFER (1986) first suggested that the phosphate anomaly (a sharp increase in concentration) is mainly the result of the redox processes involving iron and manganese responsible for the vertical transport of phosphate ions across the suboxic/anoxic interface. Thus the deeper phosphate maximum has shown a significant correlation

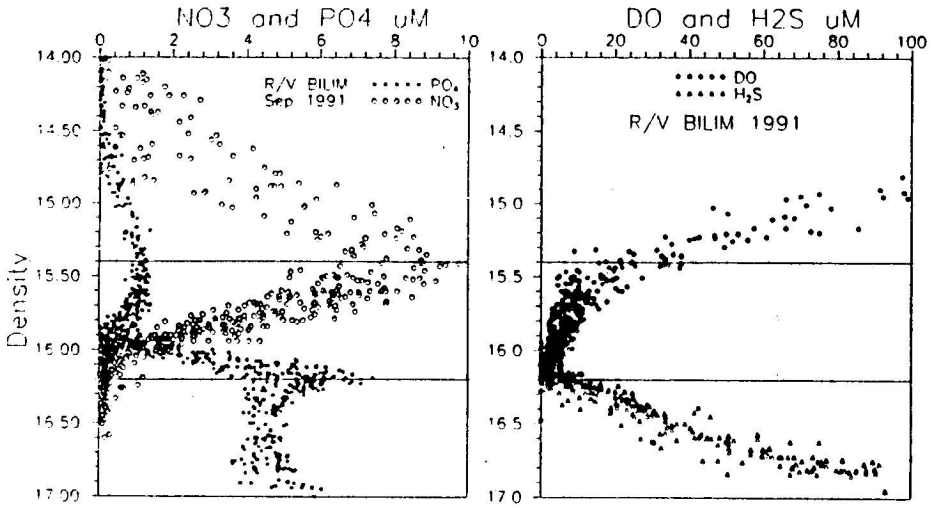

Fig. 2. Composite profiles of nitrate (NO_3), phosphate (PO_4), oxygen (DO) and hydrogen sulphide (H_2S) versus density (σ_t) for 51 stations of the R.V. *Bilim* 1991 cruise. Density is given in terms of kg m^{-3}, and others by μM.

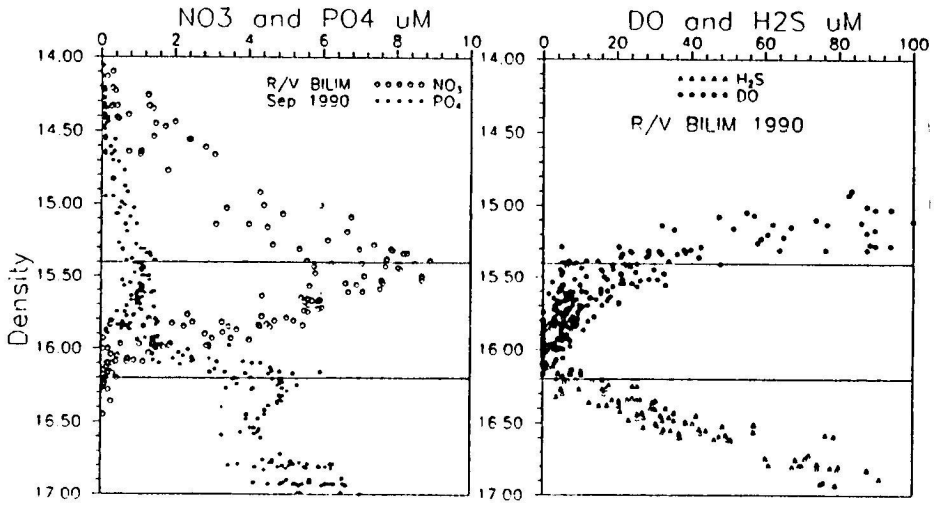

Fig. 3. Composite profiles of nitrate (NO_3), phosphate (PO_4), oxygen (DO) and hydrogen sulphide (H_2S) versus density (σ_t) for 26 stations of the R.V. *Bilim* 1990 cruise. Density is given in terms of kg m^{-3}, and others by μM.

with that of the sulphidic boundary across the basin although its depth varies markedly in space and time associated with the circulation and hydrography.

Similar composite profiles of the DO, H_2S, nitrate and phosphate concentrations for the September 1991 and September 1990 R.V. *Bilim* surveys (Figs 2 and 3) provide a confirmation for the presence of the oxic/anoxic interface zone between similar density

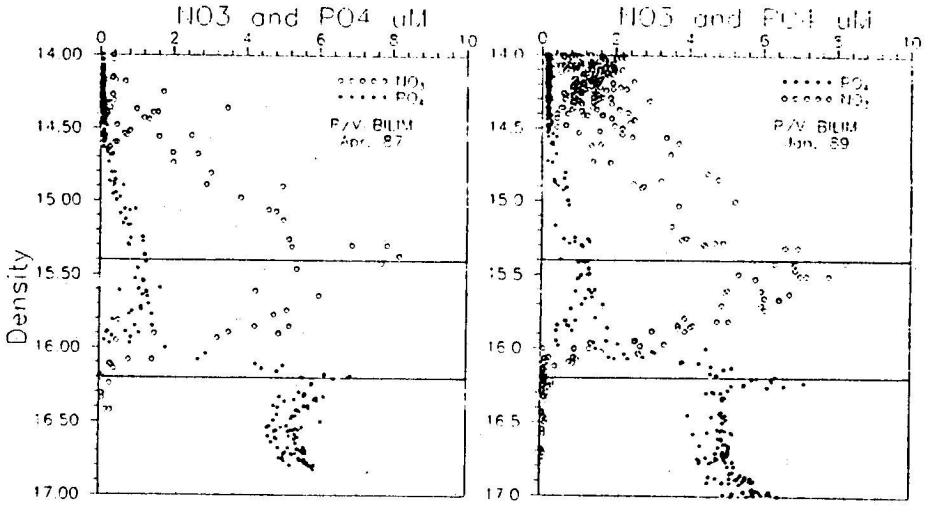

Fig. 4. Composite profiles of nitrate (NO_3), phosphate (PO_4) versus density (σ_t) for the R.V. *Bilim* April 1987 at 17 stations (left) and R.V. *Bilim* January 1989 at 24 stations (right) surveys. Density is given in terms of kg m^{-3}, and NO_3 and PO_4 by μM.

surfaces found earlier by means of the R.V. *Knorr* data. As in the previous case, the nitrate concentrations reach the maximum at $\sigma_t \sim 15.40 \pm 0.10$ at which the DO concentrations drop to the values $\sim$<20 μM from about 100 μM at $\sigma_t \simeq 15.0$. As compared with the *Knorr* 1988 data, relatively higher DO concentrations measured in the suboxic zone seem to suggest overestimation of the DO values by at least 5 μM due to air contamination during sampling from Rosette bottles.

Figures 2 and 3 also show that the phosphate anomaly is formed at a narrow range of density surfaces, similar to that in Fig. 1. Once again, the deeper phosphate maximum appears at $\sigma_t \simeq 16.20 \pm 0.05$ throughout the Black Sea, and coincides with the beginning of the anoxic sulphidic layer identified here by the H_2S concentrations of about 5 μM.

Further confirmation of the correlations between the nitrate, phosphate maxima and the boundaries of oxic/anoxic interface comes from the R.V. *Bilim* data obtained in April 1987 and January 1989 (no DO and H_2S data available) and from the Soviet R.V. *Dm. Mendeleyev* survey in August 1989 (Figs 4 and 5). Although there are relatively few data for nitrate and phosphate profiles, it is still possible to observe the nitrate maximum and the phosphate anomaly at nearly identical range of density surfaces. In the R.V. *Dm. Mendeleyev* data the DO and H_2S concentrations (Fig. 5), confined within these density surfaces, are considerably higher compared with other data sets presented in Figs 1–3. We note that DO concentrations in this transitional layer may be as high as approximately 20 μM. This may suggest a higher degree of atmospheric contamination and the subsequently apparent observation of the C-layer, i.e. DO and H_2S are overlapped in the oxic/anoxic interface zone. Air contamination is clearly shown in Fig. 5 by the presence of DO concentration of about 10 μM within the anoxic layer.

Other scientific evidence for the possible use of the certain density levels for delineating the boundaries of the oxic/anoxic interface zone is provided by the light transmission measurements of the R.V. *Knorr* 1988 cruises (WHITE *et al.*, 1989). These measurements reveal the existence of a minimum formed consistently at $\sigma_t \sim 16.1$–16.2 and subsequent

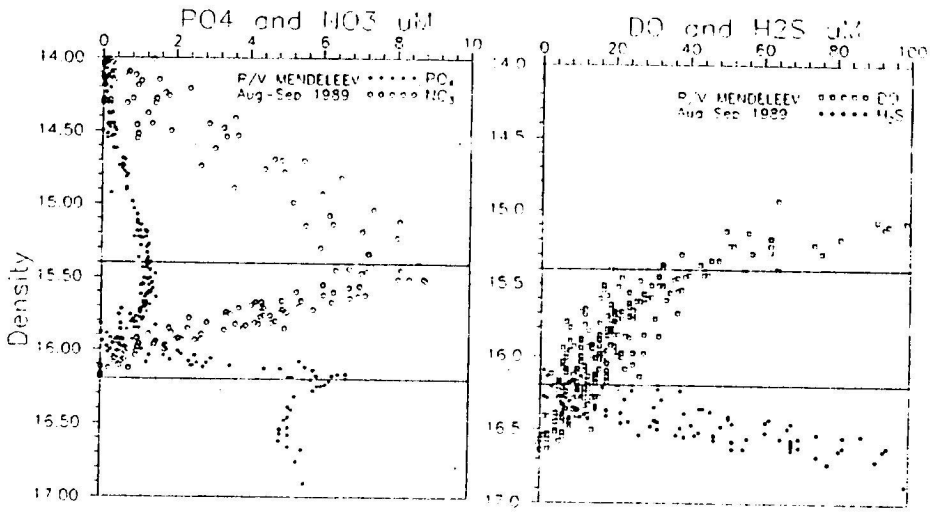

Fig. 5. Composite profiles of nitrate (NO_3), phosphate (PO_4), oxygen (DO) and hydrogen sulphide (H_2S) versus density (σ_t) for 15 stations of the R.V. *Dm. Mendeleyev* 1989 cruise. Density is given in terms of kg m^{-3}, and others by μM.

increase to the background levels at $\sigma_t \sim 16.20 \pm 0.05$. The decrease in the intensity of light transmission is associated with the Fine Particle Layer (FPL) observed by KEMPE *et al.* (in press) at the same range of the density surfaces. The FPL most probably originates from the remobilized Mn and Fe particles (KEMPE *et al.*, in press) as well as the particulate organic matter chemosynthetically produced immediately above the anoxic sulphidic layer (SAPOZHNIKOV *et al.*, 1985). The base of the peaks in the light transmission, therefore, corresponds to the sulphide bearing lower boundary of the suboxic zone below which the Mn and Fe oxyhydroxides will dissolve (SHAFFER, 1986) due to the decreases in the redox potential. We note that the formations of both the FPL and phosphate minimum and their interactions are not yet fully understood because of the complicated biogeochemical processes taking place in the transitional zone.

The confinement of the suboxic zone between fixed density levels, of course, does not mean that this layer remains constant at the same depths throughout the entire basin. Figure 6a,b shows the distribution of $\sigma_t = 15.40$ and $\sigma_t = 16.20$ surfaces, respectively, for the September 1990 survey to the east of 32°E longitude. It is evident that the location of the $\sigma_t = 15.40$ surface varies from 70 to 125 m within the basin in accordance with the general circulation in the region (OGUZ *et al.*, in press). It is shallower in the cyclonic regions and deeper in the anticyclonic regions, with most pronounced variations taking place along the rim current encircling the periphery of the basin. The $\sigma_t = 16.20$ surface also has similar characteristics, varying between 120 and 165 m at the centers of the cyclonic and anticyclonic eddies, respectively. Contrary to the pronounced horizontal variability of the boundaries of the transitional layer, Fig. 6a,b suggests that this layer has a constant thickness of about 50 m. In fact, the average thickness for the entire data set amounts to 52 ± 7 m. A relatively deeper suboxic layer is situated in the regions of anticyclonic eddies (generally along the coast) as compared to the shallower layer in the cyclonically-dominated regions (usually within the interior of the basin). These are further

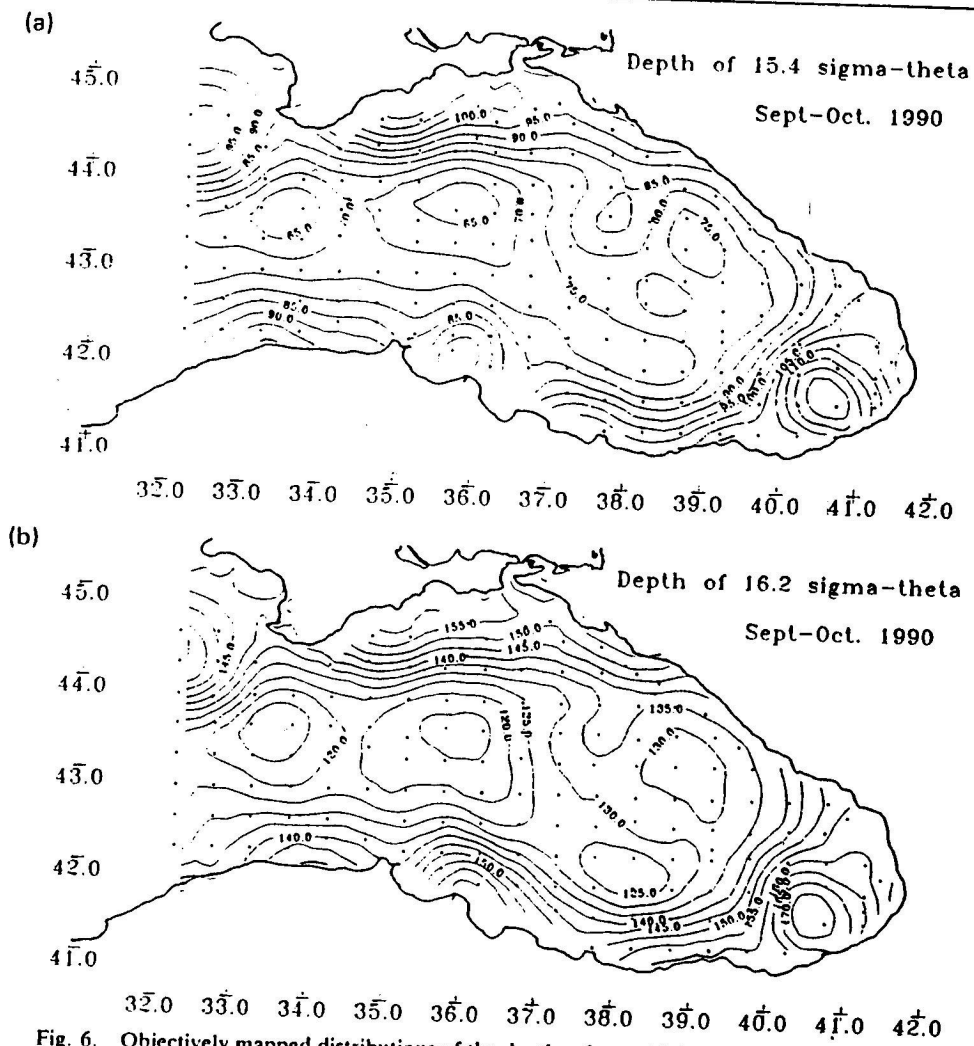

Fig. 6. Objectively mapped distributions of the depths of σ_t = 15.4 density surface for the joint cruise of the R.V. *Bilim* and R.V. *Lomonosov* in September–October 1990. Contour interval is 5 m. The station locations are shown by dots. (b), Same as (a) for the depths of σ_t = 16.2 density surface.

supported by other R.V. *Bilim* cruises conducted during 1987–1991, although they all have different numbers of sampling stations and locations.

Acknowledgements—This work is supported by the Turkish Scientific and Technical Research Council (TUBITAK) under the National Black Sea Oceanographic Programme. Support is also given by the NATO Science For Stability Programme–Black Sea Fisheries Project. We would like to thank those scientists, technicians and crew members who took part during the surveys of R.V.'s *Bilim*, *Knorr* and the *Dm. Mendeleyev*. We also kindly acknowledge the U.S. and Soviet scientists who provided us with all the hydrochemical data of the joint cruises of R.V. *Knorr* (1988) and the R.V. *Dm. Mendeleyev* (1989) and R.V. *Lomonosov* (1990). The authors wish to thank S. Tont for his thorough reading of the paper, and his helpful comments.

REFERENCES

BRYANTSEV V. A., D. YA. FASCHUK, T. A. AYZATULLIN, S. V. BAGOTSKY and V. A. LEONOV (1988) Variation in the upper boundary of the hydrogen sulphide in the Black Sea: analysis of field observations and modelling results. *Oceanology*, **28**, 180–185.

CODISPOTI L. A., G. E. FRIEDERICH, J. W. MURRAY and C. M. SAKAMOTO (1991) Chemical variability in the Black Sea: implications of continuous vertical profiles that penetrated the oxic/anoxic interface. *Deep-Sea Research*, **38**, Suppl.2, S691–S710.

FREDERICH G. E., L. A. CODISPOTI, C. M. SAKAMOTO (1990) Bottle and pumpcast data from the 1988 Black Sea expedition. Technical Report No. 90-3, Montery Bay Aquarium Research Institute.

GRASSHOFF K. (1975) The hydrochemistry of landlocked basins and fjords. In: *Chemical oceanography*, J. P. RILEY and C. SKIRROW, editors, Academic Press, New York, pp. 456–597.

KEMPE S., G. LIEBEZEIT and A. R. DIERCKS (1990) Water balance in the Black Sea. *Nature*, **346**, pp. 419.

KEMPE S., A. R. DIERCKS, G. LIEBEZEIT and A. PRANGE (1991) Geochemical and structural aspects of the pycnocline in the Black Sea (R.V. *Knorr* 134-8 LEG 1, 1988). In: *Black Sea oceanography*, E. IZDAR and J. W. MURRAY, editors, NATO ASI Series, Kluwer, Deventer, pp. 89–110.

MILLERO F. J. (1991) The oxidation of H_2S in the Black Sea waters. *Deep-Sea Research*, **38**, Suppl. 2, S1139–S1150.

MURRAY J. W. and E. IZDAR (1989) The 1988 Black Sea oceanographic expedition: overview and new discoveries. *Oceanography*, **2**, 15–21.

MURRAY J. W., H. W. JANNASCH, S. HONJO, R. F. ANDERSON, W. S. REEBURGH, Z. TOP, G. E. FRIEDERICH, L. A. CODISPOTI and E. IZDAR (1989) Unexpected changes in the oxic/anoxic interface in the Black Sea. *Nature*, **338**, 411–413.

MURRAY J. W., Z. TOP and E. OZSOY (1991) Hydrographic properties and ventilation of the Black Sea. *Deep-Sea Research*, **38**, Suppl. 2, S663–S690.

OGUZ T., M. A. LATIF, H. I. SUR, E. OZSOY and U. UNLUATA (1991) On the dynamics of the southern Black Sea. In: *Black Sea oceanography*, E. IZDAR and J. W. MURRAY, editors, NATO ASI Series, Kluwer, pp. 43–63.

OGUZ T., P. LA VIOLETTE and U. UNLUATA (1992) The upper layer circulation in the southern Black Sea: its variability as inferred from hydrographic and satellite observations. *Journal of Geophysical Research*, **97**, 12569–12584.

OGUZ T., V. S. LATUN, M. A. LATIF, V. V. VLADIMIROV, H. I. SUR, A. A. MARKOV, E. OZSOY, B. B. KOTOVSHCHIKOV, V. V. EREMEEV and U. UNLUATA (in press) Circulation in the surface and intermediate layers of the Black Sea. *Deep-Sea Research I*.

SAPOZHNIKOV V. V., V. A. BIBIKOV, D. YA. FASCHUK and M. S. FINKELSTEYN (1985) A phosphate minimum in the layer of coexistence of oxygen and hydrogen sulphide in the Black Sea. *Oceanology*, **25**, 966–969.

SEITZINGER S. P. (1988) Denitrification in fresh water and coastal marine ecosystems: ecological and geochemical significance. *Limnology and Oceanography* **33**, 702–724.

SHAFFER G. (1986) Phosphate pumps and shuttles in the Black Sea. *Nature*, **321**, 515–517.

SOROKIN YU I. (1983) The Black Sea. In: *Estuaries and enclosed seas. Ecosystem of the World*, B. H. KETCHUM, editor, Elsevier, Amsterdam, **26**, 253–292.

TUGRUL S., O. BASTURK, C. SAYDAM and A. YILMAZ (1992) Changes in the hydrochemistry of the Black Sea inferred from density profiles. *Nature*, **359**, 137–139.

WHITE G., M. RELANDER, J. POSTAL and J. W. MURRAY (1989) Hydrographic data from the 1988 Black Sea oceanographic expedition. University of Washington, School of Oceanography, Report No. 109.

Deep-Sea Research II, Vol. 40, No. 6, pp. 1075–1119, 1993.
Printed in Great Britain.

0967-0645/93 $6.00 + 0.00

A synthesis of the Levantine Basin circulation and hydrography, 1985–1990

E. Özsoy,* A. Hecht,† Ü. Ünlüata,* S. Brenner,† H. İ. Sur,* J. Bishop,† M. A. Latif,* Z. Rozentraub† and T. Oğuz*

(*Received* 1 *January* 1992; *in revised form* 3 *February* 1993; *accepted* 26 *February* 1993)

Abstract—The Levantine Basin circulation derived from recent data consists of a series of sub-basin-scale to mesoscale eddies interconnected by jets. The basin-scale circulation is masked by eddy variability that modulates and modifies it on seasonal and interannual time scales. Long-term qualitative changes in the circulation are reflected in the bifurcation patterns of the mid-basin jets, relative strengths of eddies and the hydrographic properties at the core of these eddies. Confinement within the Basin geometry strongly influences the co-evolution of the circulation features.

Surface measurements, satellite images and the mass field indicate an entire range of scales of dynamical features in the region. The complexity of the circulation is consistent with the basin-wide and mesoscale heterogeneity of the hydrographic properties. The interannual variability of LIW (Levantine Intermediate Water) formation in the region appears correlated with the changes in the circulation. Wintertime convective overturning of water masses reach intermediate depths and constitute a dominant mechanism of LIW formation, especially in anticyclonic eddies and along the coasts of the northern Levantine Basin.

1. INTRODUCTION

Recent observations, made possible through the national programmes of bordering countries and planning under the POEM research programme (Physical Oceanography of the Eastern Mediterranean, Unesco, 1984, 1985, 1987; Malanotte-Rizzoli and Robinson, 1988; Özsoy *et al.*, 1989, 1991; Robinson *et al.*, 1991a; The POEM Group, 1992), have made significant contributions to a much needed understanding of the Eastern Mediterranean circulation.

In the past, the lack of a coherent description of the circulation and water mass production in the Eastern Mediterranean often has been attributed to the insufficient data base (e.g. Malanotte-Rizzoli and Hecht, 1988). Today, we begin to recognize complexity and natural variability as inherent properties of the system, making their scientific understanding difficult but rewarding.

Conflicting hypotheses have emerged, especially with regard to the Levantine Basin dynamics. For many years, the traditional Nielsen (1912) scheme of a cyclonic circulation along the coasts of the Levantine Basin has only undergone minor modification, e.g. a bifurcation of the currents sweeping the island of Cyprus (Lacombe, 1975). The data from intensive investigations till the end of the 1960s (Ovchinnikov, 1966; Ovchinnikov *et al.*,

*Institute of Marine Sciences, Middle East Technical University, P.K. 28, Erdemli, İçel, 33731 Turkey.
†Israel Oceanographic and Limnological Research Ltd., Tel Shikmona, Haifa, 31080 Israel.

1976) did not alter the basic Nielsen concept. However, Ovchinnikov (1966) did indicate a small anticyclonic gyre in the southwest Levantine. In fact, data obtained in the 1970s (e.g. Ovchinnikov *et al.*, 1976; Ovchinnikov, 1984a; Engel, 1967; Oren, 1970) indicated various anticyclonic eddies in the southern part of the Levantine basin, but these findings did not gain sufficient recognition. The five year "Marine Climate" (MC) program (Hecht *et al.*, 1988) also indicated anticyclonic circulations in the southeastern Levantine, and showed a complex system of mesoscale eddies, jets and patches of water masses embedded in the general circulation.

The cyclonic Rhodes Gyre was recognized as the dominant circulation in the area between Crete and Cyprus (e.g. Ovchinnikov, 1966; Phillippe and Harang, 1982; Anati, 1984), but persistent anticyclonic eddies were later found on its periphery (Özsoy *et al.*, 1989, 1991; Robinson *et al.*, 1991a).

More recent analyses of the historical data (Feliks and Itzikowitz, 1987) and inverse models of the climatological mean circulation (Tziperman and Malanotte-Rizzoli, 1991) reveal an abundance of anticyclonic eddies in the Levantine Basin outside the zone of influence of the Rhodes Gyre.

The combined data of the Israeli R.V. *Shikmona* and the Turkish R.V. *Bilim* provided unique details of Levantine Basin circulation (Özsoy *et al.*, 1989, 1991) which differed significantly from the earlier descriptions (e.g. Ovchinnikov *et al.*, 1976) and consisted of quasi-permanent sub-basin-scale gyres, eddies, and intense mid-basin jets. The Atlantic and Levantine Intermediate waters were shown to survive the seasonal cycles of formation and advection and to become entrained into eddies. The collective data base (The POEM Group, 1992; Robinson *et al.*, 1991a) extended these results to the description of the Eastern Mediterranean general circulation.

The northern Levantine Basin, driven by surface buoyancy fluxes (Morcos, 1972), is identified as the main source region of LIW. On the other hand, the basin-wide heterogenous distribution and year-around persistence (Özsoy *et al.*, 1989) of the LIW point to the role of interior dynamics in maintaining it.

The complexity of the basin dynamics has precluded the construction of a valid and simple theory for LIW formation. The following basic hypotheses have been advanced to date: (i) isopycnal sinking into the adjacent anticyclonic eddies of dense surface water formed by convection in cyclonic regions, e.g. Rhodes Gyre (Ovchinnikov, 1984b; Ovchinnikov and Plakhin, 1984); (ii) continental shelf/slope convection processes in the adjacent Aegean Sea (Bruce and Charnock, 1965; Georgopoulos *et al.*, 1989); (iii) local convective overturning preferentially occurring in anticyclonic eddy centers (Brenner *et al.*, 1991); (iv) Ekman flux accumulation near the coast of water formed by basin-wide wind-induced mixing (Feliks, 1991); and (v) massive formation in the entire northern Levantine by convective overturning due to rare, interannual cooling–wind mixing events (Sur *et al.*, 1993).

In the following discussion, we emphasize the seasonal and interannual variability of the Levantine Basin circulation, presenting pertinent and new results for the 1985–1990 period.

2. SOME REGIONAL CHARACTERISTICS

2.1. *Bottom topography*

The deep Hellenic Trench encircles the northern Cretan Passage, with deepest points occurring at the Rhodes Basin (Fig. 1). The Mid-Mediterranean Ridge running from the

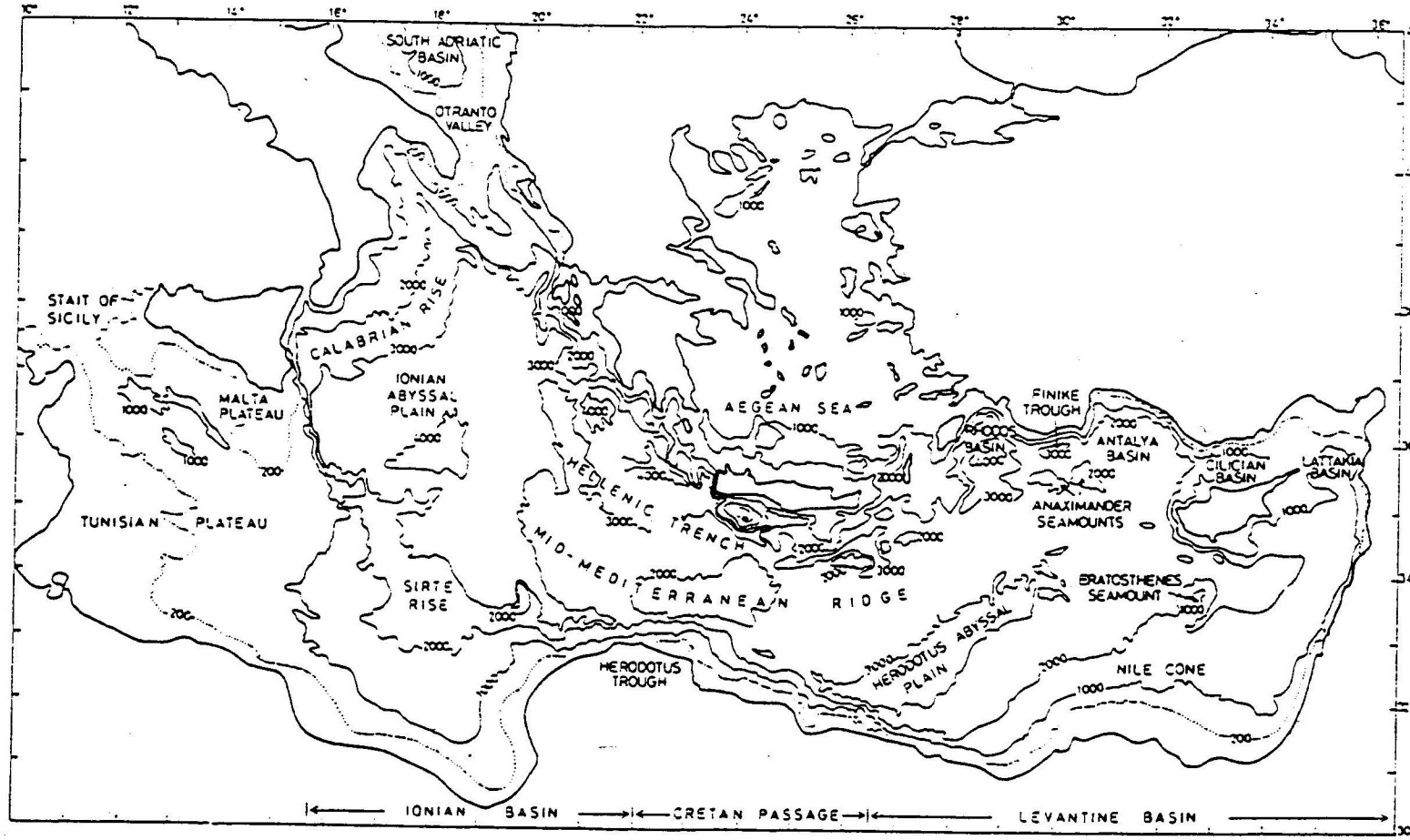

Fig. 1. Location map and bathymetry of the Eastern Mediterranean, including the Levantine Basin.

Ionian Basin into the Levantine Basin is shallowest along the Herodotus Rise (1600 m). The Herodotus Trough extends along the southern part of the Cretan Passage, and the Herodotus Abyssal Plain (3000 m) occupies southwestern Levantine Basin. The island of Cyprus adjoins shallow topography in the northeastern corner.

The smaller scale bathymetric features of the Levantine Basin are the Lattakia (1000–1500 m), Cilician (1000 m), Antalya (2000–3000 m) and Rhodes (4300 m) Basins and the Anaximander (1500 m) and Eratosthenes (1000 m) Seamounts. The relatively shallow Lattakia and the Cilician Basins communicate with each other through a narrow channel of 700 m depth located nearly midway between the sill between Cyprus and the Gulf of İskenderun (Fig. 1).

2.2. *Climate*

Winter and spring extratropical cyclones intensifying in the Cyprus area create significant space–time variability in the meteorological conditions (Reiter, 1975; Brody and Nestor, 1980; Özsoy, 1981), leading to local wind systems driven by the compounding effects of climatic contrasts and land topography. Some examples are Sirocco and Khamsin along the African coast, Etesians over the Aegean Sea and Poyraz along the Anatolian coast (Reiter, 1975; Özsoy, 1981). In addition, intense sea-breezes in summer and autumn accompany the seasonal wind systems.

Climatological wind fields basically can be described in the form of predominant westerlies in winter, and northwesterlies strengthened by the Aegean Etesian regime in summer (Middelandse Zee, 1957; Brody and Nestor, 1980; May, 1982). The outbreaks of cold and dry air into the Eastern Mediterranean from the northern continental regions play important roles in the oceanography of the region, leading to significant buoyancy losses initiating the formation of the Levantine Intermediate Water (Wüst, 1961; Morcos, 1972).

Estimates of fluxes at the air–sea interface and climatological data have been used in the numerical model studies of Pinardi and Navarra (1988, 1991), Malanotte-Rizzoli and Bergamasco (1989, 1991) and Bergamasco *et al.* (1993). According to these studies, the surface fluxes are important, but not necessarily in direct correlation with the circulation. For a review of the climatology data, the reader is referred to these references and to Özsoy *et al.* (1989) and Özsoy and Ünlüata (1993).

3. THE DATA SETS AND METHODS OF ANALYSES

The Levantine Basin data were obtained from a number of oceanographical cruises of the participating institutions (Table 1). The most complete coverage of the Basin was obtained in the POEM01 (October–November 1985), POEM02 (March–April 1986) and POEM05 (August–September 1987) surveys (Özsoy *et al.*, 1989, 1991; The POEM Group, 1992; Robinson *et al.*, 1991a). During POEM05 (August–September 1987), multiship cruises covered the Eastern Mediterranean, but due to technical problems, the R.V. *Bilim* data extended only up to a depth of 500 m and the R.V. *Shikmona* could not finish the planned number of stations. Due to recovery problems of the CTD data, only bottle data were used from the R.V. *Shikmona* (Pinardi, 1988; Özsoy *et al.*, 1991); in the present analyses the original CTD data are used. A separate survey (POEM06) was jointly carried

Table 1. *Levantine Basin oceanographic cruises* 1985–1992

Cruise	Dates	Ships	Coverage	Number of Sations
POEM01	Oct–Nov 1985	*Bilim* and *Shikmona*	LB	124
POEM02	Mar–Apr 1986	*Bilim* and *Shikmona*	LB	99
—	Jun 1986	*Bilim*	north LB	93
—	Nov 1986	*Bilim*	north LB	16
POEM04	Feb 1987	*Bilim*	north LB	34
—	Jun 1987	*Bilim*	north LB	75
POEM05	Aug–Sep 1987	*Bilim* and *Shikmona*	LB	117
—	Jan 1988	*Bilim*	north LB	18
—	May 1988	*Bilim*	north LB	19
POEM06	Jul 1988	*Bilim* and *Shikmona*	LB	128
—	Oct 1988	*Bilim*	north LB	58
—	Nov 1988	*Bilim*	north LB	14
—	Feb 1989	*Bilim*	north LB	6
LBDS01	Mar 1989	*Bilim* and *Shikmona*	LB	163
—	Aug 1989	*Bilim*	north LB	14
—	Oct 1989	*Bilim*	north LB	12
—	Mar 1990	*Bilim*	north LB	28
LBDS02	Aug 1990	*Bilim*	north LB	58
LBDS02	Aug 1990	*Shikmona*	south LB	109
—	Nov 1990	*Bilim*	north LB	57
—	Mar 1991	*Bilim*	north LB	50
LBDS03	Oct–Nov 1991	*Bilim* and *Shikmona*	LB	167
—	Mar 1992	*Bilim*	north LB	50

out by the IMS-METU and the IOLR during July–August 1988; its combined data are also analysed in the present work.

After the POEM experiments, basin-wide surveys were continued in the context of the Levantine Basin Dynamical Studies (LBDS), with the collaboration of IMS-METU (Institute of Marine Sciences of the Middle East Technical University), IOLR (Israel Oceanographic and Limnological Research), and Harvard University. Extensive coverage of the Basin was obtained in March 1989 (LBDS01), August 1990 (LBDS02) and October–November 1991 (LBDS03). A number of other cruises (Table 1) carried out by the R.V. *Bilim* in the northern Levantine Basin were less extensive, but valuable interpretations from these data sets have been included as necessary, to bridge the gaps in coverage.

The instruments and the data processing/analysis techniques are described in Özsoy *et al.* (1989). Corrections of $\Delta T = +0.04, +0.02, 0.0, +0.01$, and $\Delta S = +0.03, +0.06, -0.04, +0.06$ were applied to the R.V. *Bilim* data for the combined data sets of October–November 1985, March–April 1986, August–September 1987, and March 1989 data sets, respectively, based on measurements at intercalibration stations (excluding August–September 1987, for which intercalibrations were carried out between pairs of POEM05 data sets, Pinardi, 1988). For the other R.V. *Bilim* data no calibrations could be made because no other independent data were available.

A reference level of 800 dbar was used in dynamical computations, excluding June 1987 (650 dbar) and August–September 1987 (450 dbar), when the depth of the R.V. *Bilim* data was limited. The dynamic height is calculated in cm units, and the observational mean is

subtracted. The objective analyses are made on a regular grid of (1/4)° spacing, using a correlation model fitted to the observations. The gridded data are contoured by the ZCSEG contouring routine of the PLOT88 Library (Plotworks Inc.), with four grid subdivisions and two subsegments for each linear contour segment. The contouring is masked by coastal boundaries and when the normalized error variance exceeds 0.6.

During the surface sampling program of the R.V. *Bilim* in October–November 1985, temperature and salinity were subsampled at 5 min intervals from continuous measurements of the CTD placed in a container pumped with seawater from below the surface (depth ~5 m) and phosphate samples were collected at every 20–30 min intervals. Because of calibration problems of the analysis technique used, the phosphate measurements were biased (an order higher than the levels obtained in later measurements), but we present them in a qualitative manner because they are the only continuous surface measurements we have made to date.

The Channel 4 AVHRR satellite data in Section 5 were obtained from the NOAA-10 and NOAA-11 satellites, and were processed for atmospheric corrections, Mercator map projections, and contrast stretching at the IMS-METU using the SEAPAK system (McClain *et al.*, 1992).

4. THE BASIN CIRCULATION AND ITS VARIABILITY

The motions in the Levantine Basin are characterized by a wide range of scales. Confinement of the motions within the Levantine Basin boundaries leads to basin-wide or sub-basin-scale dynamical structures and eddies with coarse mesoscale dimensions (50–100 km) often mask these features. In addition, mesoscale (internal radius of deformation ≈ 10–15 km) and sub-mesoscale features are often identified in high resolution surface and subsurface data (Özturgut, 1976; Özsoy *et al.*, 1986; Robinson *et al.*, 1987; The POEM Group, 1992) and in satellite images (Section 5), but cannot be resolved by the nominal spacing [of (1/2)° ≈ 50 km] of the CTD stations used in the present surveys. Low-frequency (shelf and basin modes with periods of several days to weeks) and high-frequency (diurnal, inertial and shorter periods) current oscillations, superposed on mean westerly currents have been measured along the Turkish continental shelf in the Cilician Basin (Özsoy and Ünlüata, 1992).

The time scales of the coarse mesoscale and sub-basin-scale motions resolved by the dynamical calculations are typically of the same order as the time interval between surveys. The large coherent eddies and gyres survive sufficiently long to make comparisons between cruises possible. Brenner *et al.* (1991) and Brenner (1993) have shown long-term persistence of the Shikmona eddy, despite changes in its structure and position. Preliminary numerical experiments also have indicated long-lived structures in the flow field in the absence of surface forcing (Robinson *et al.*, 1991b; Özsoy *et al.*, 1990, 1992).

The first basin-wide data set, obtained in October–November 1985, (POEM01), demonstrates the major elements of the Levantine Basin circulation (Özsoy *et al.*, 1989): the Rhodes Gyre, its multiple centers southeast of the island of Rhodes and extension towards Cyprus; the intense Mersa Matruh Gyre south of the Rhodes Gyre; the Shikmona Gyre complex with a number of separate centers in the southeastern Levantine Basin; and a coherent mid-basin jet, identified as the Central Levantine Basin Current, flowing eastwards amongst these vortices [Fig. 2(a)]. On its course, the Central Levantine Basin Current bifurcates and becomes entrained in the sub-basin-scale gyres. At the first

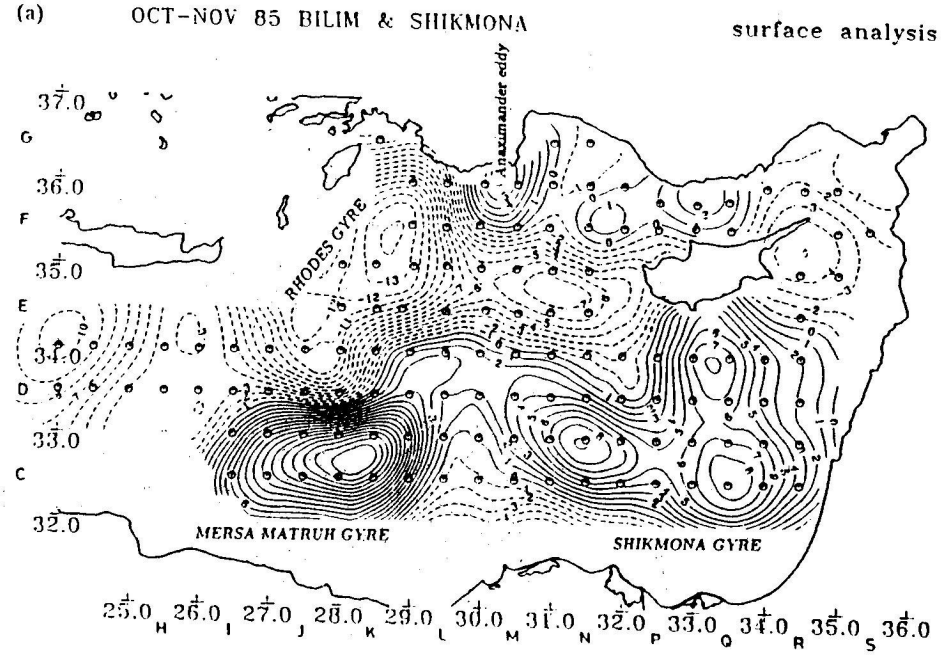

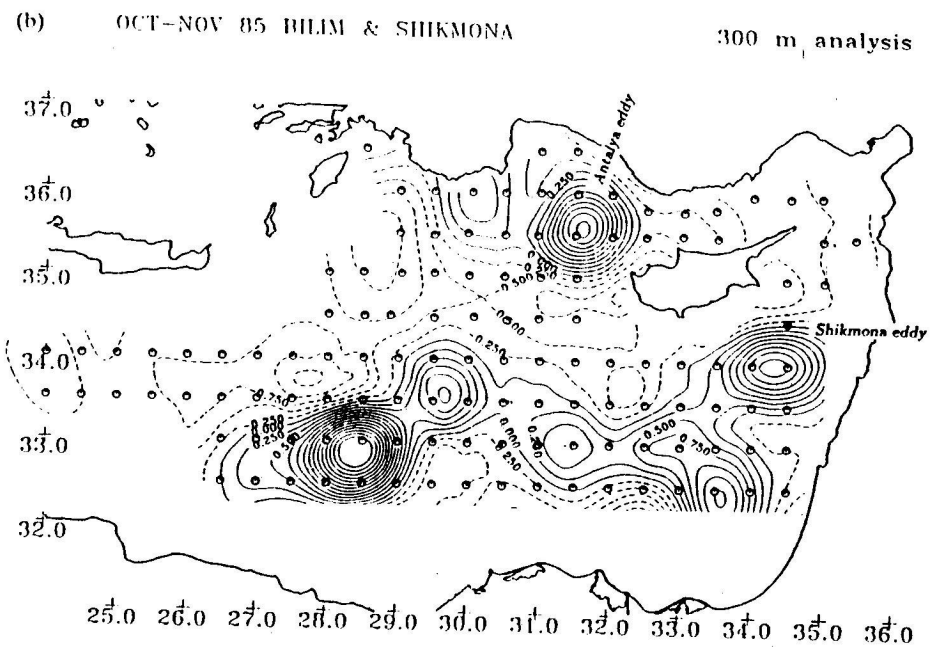

Fig. 2. (a) Surface and (b) 300 db dynamic height (in cm) referenced to 800 decibar level of no motion, October–November 1985. The one degree square letter coding used in station naming convention is also shown along the latitude and longitude divisions.

bifurcation, the jet partly encircles the Mersa Matruh Gyre and partly flows around the Rhodes Gyre eventually to join with the westerly flow (the Asia Minor Current) along the southwest Anatolian coast. The remaining core of the jet divides once more southwest of Cyprus, with the branches following the Rhodes Gyre extension and southern Cyprus.

The persistence and continuity of the Central Levantine Basin Current are not well-defined despite the new data sets. The current system can not be separated from the gyres and the eddy field that partly define it. The Central Levantine Basin Current (i.e. the Mid-Mediterranean Jet of Robinson *et al.*, 1991a), the Ionian Atlantic Stream issuing from the Straits of Sicily (Robinson *et al.*, 1991a), and currents along the Cyrenaican coast (e.g. Phillippe and Harang, 1982) could all be different parts of a continuous current, i.e. the North African Current as visualized by Ovchinnikov (1966), but the POEM data coverage in the south Ionian Sea is insufficient to establish the connection between them (Robinson *et al.*, 1991). At the Strait of Sicily, estimates of the surface inflow carrying an influx of Atlantic Water (AW) into the Eastern Mediterranean, and the deeper flow exporting Levantine Intermediate Water (LIW) to the west vary from 1 *Sv* (= 10^6 m^3 s^{-1}) (either way; Garzoli and Maillard, 1979) to a seasonal range of 1.5 *Sv* (summer) to 3 *Sv* (winter; Manzella *et al.*, 1988).

The exact nature of the return flows of the mid-basin jet is also not well known. One branch of the return flow, the Asia Minor Current, persists for part of the observation period (below). The flow along the southern coast is less certain due to observational difficulties along the shallow Nile Cone topography, but continuity would require westward flow, in conflict with earlier estimates (e.g. Ovchinnikov, 1966). We also note

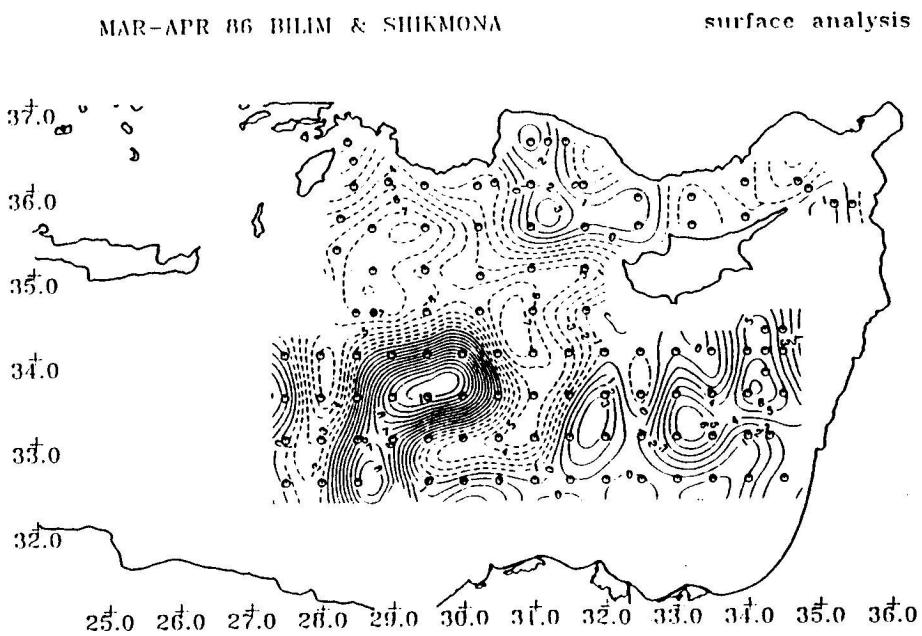

Fig. 3(a).

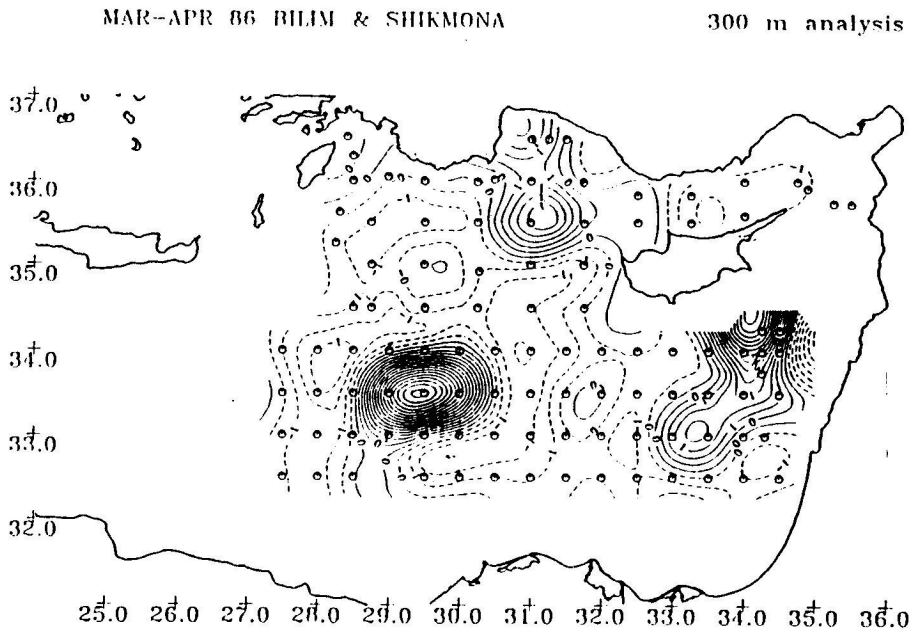

(b)

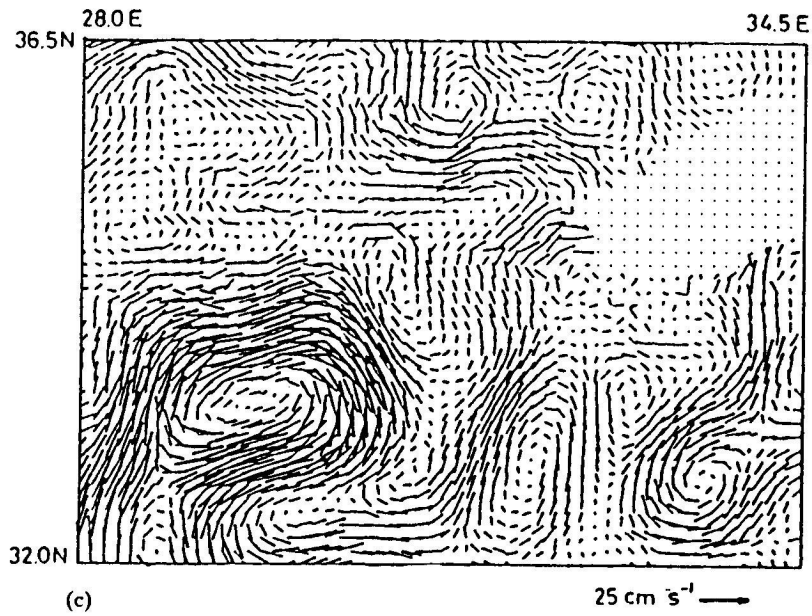

(c)

Fig. 3. (a) Surface and (b) 300 db dynamic height (in cm) referenced to 800 decibar level of no motion; (c) surface currents, March–April 1986.

that some of the return flow could be incorporated into the vertical circulation of the Basin. The volume fluxes through the Sicily Strait are of the same order of magnitude as the fluxes recirculating around typical sub-basin gyres, and much greater than the surface fluxes, so that a vertical circulation is required for a balance. They could also be driven by thermohaline (surface or Strait buoyancy fluxes) or wind (area-integrated Ekman flux divergence) effects. Robinson *et al.* (1991a) have constrained their analyses with the zero normal flux condition along hypothetical boundaries (the 600 m depth contour), but have found different streamfunction values along the southern and northern boundaries of the Levantine Basin, confirming an unbalanced net flux of the mid-basin currents. In our analyses, we prefer to leave the analyses unconstrained at the coast, but observe that the coastal features such as the Asia Minor Current are better resolved by the data when these flows are sufficiently developed.

A persistent anticyclonic feature (the Anaximander eddy) appears between the Anaximander Seamounts and the Anatolian coast (Fig. 1). Another one (the Antalya anticyclonic eddy) occupies the western entrance to the Cilician Basin from the Antalya Basin. The Anaximander eddy becomes weaker at 300 m [Fig. 2(b)], while the Antalya eddy is intensified to become a coherent feature at intermediate depth. The other coherent features at 300 m are the twin centers of the Mersa Matruh Gyre and the northerly member of the Shikmona Gyre complex.

In the following March–April 1986 (POEM02) survey, the Rhodes, the Mersa Matruh, and the Shikmona Gyres survive the winter, despite changes in form [Fig. 3(a)]. The crescent shaped Rhodes Gyre is observed to engulf the Mersa Matruh Gyre. The Central Levantine Basin Current has a meandering structure following the common boundary of the Mersa Matruh and Rhodes Gyres. It makes wide north–south excursions extending first from Crete to the African coast, then to mid-basin and back to the African coast and finally to the Anatolian coast following the periphery of the Rhodes Gyre. The Central Levantine Basin Current of the POEM01 analyses seems to have broken into two loops, one completing the circuit just described, and the other encircling the Shikmona Gyre in the east. Incipient breakdown of the meandering jet flow into separate loops appeared at other places, i.e. near 35°N 30°E, where a deep structure was found inside the narrowing region of the cyclonic Rhodes Gyre (Fig. 17, Özsoy *et al.*, 1989). The closed anticyclonic contours in Fig. 3(b) may reflect such breakdown, in spite of the coarse station spacing. The surface currents computed for a limited rectangular subdomain in Fig. 3(c) show intense currents along the periphery of the various mid-basin gyres.

Two eddy centers appear in an anticyclonic circulation cell in Antalya Bay [Fig. 3(a)]. At depth [Fig. 3(b)], one of these intensifies relative to the other, and could correspond to the Antalya anticyclone, with its center shifted west from its earlier position [Fig. 2(b)]. Coherent anticyclonic vortices are also identified within the Mersa Matruh and Shikmona Gyres [Fig. 3(b)].

During June 1986 (not shown), the Anaximander and Antalya anticyclones persisted along the Anatolian coast. The Antalya anticyclone had an intense deep structure [Fig. 13(b); Özsoy *et al.*, 1991].

In the October–November 1985, March–April 1986 and June 1986 surveys, weak counter-rotating circulations were found in the Lattakia and Cilicia Basins, indicating limited penetration of the mid-basin mainstream flows into the region blocked by the island of Cyprus. The main features of the general circulation persisted during a rather long period in 1985–1986, despite deformations and dispersion. One of the characteristi-

cally long-lived members of this circulation was the Antalya anticyclone, which survived in nearly the same position.

In the following period of winter 1986–1987, qualitative changes could be traced in the northern Levantine circulation. First, two small anticyclonic eddies arrived from the south into the Lattakia Basin in February 1987, transporting AW with them [Fig. 13(c); Özsoy *et al.*, 1991]. The following June 1987, the pattern of circulation changed significantly [Fig. 4(a) and (b)], and AW flooded the northern region [Fig. 13(d); Özsoy *et al.*, 1991]. The Cilicia and Lattakia Basins were occupied by a number of anticyclonic eddies that seemed related to those entering in February 1987. The Rhodes Gyre extension retreated west, and an anticyclonic eddy, possibly formed by a merger of the Anaximander and the Antalya anticyclonic eddies, occupied the west side of the Antalya Basin. There seems to be some parity between the Anaximander and Antalya anticyclones: interactions seem to occur between them leading to the shifts in March–April 1986 and June 1987. In the former event the water mass signature inside the eddies was preserved (Özsoy *et al.*, 1991), and in the latter case it was radically altered (Section 6.1).

It is interesting to note that during the same period in 1987, Gertman *et al.* (1990) observed deep water formation in the Rhodes Gyre region (Section 6.3), a previously unknown and rare event which may have triggered the subsequent changes in the circulation. The February 1987 cruise of the R.V. *Bilim* was discontinued west of Antalya Bay due to bad weather.

In August–September 1987 (POEM05), the Rhodes Gyre extended into the Antalya Basin, and the weak anticyclonic circulation persisted in the Cilician Basin [Fig. 5(a)]. The Antalya anticyclonic eddy either completely disappeared or perhaps had been replaced by the Anaximander eddy. In the southern part of the basin, Mersa Matruh and Shikmona Gyre complexes persisted. The Shikmona eddy shifted south (Brenner *et al.*, 1991) and had an intense signature at 300 m depth [Fig. 5(b)]. The other features at depth were the small Anaximander and northeast Cyprus anticyclonic eddies.

Based on the larger set of POEM05 data in the region, The POEM group (1990) and Robinson *et al.* (1991a) identified a bifurcating Central Levantine Basin Current south of the Rhodes Gyre, with one branch proceeding northeastward and then westward along the periphery of the Rhodes Gyre, the other branch flowing south of Cyprus and then southward around the Shikmona Gyre. None of the Central Levantine Basin Current waters seemed to penetrate into the Cilician Basin.

Combined data of July 1988 (POEM06) reveal significant changes with respect to the earlier circulation patterns [Fig. 6(a)]. The Rhodes Gyre covers an extensive area and engulfs an anticyclonic eddy to its south. The Shikmona Gyre complex covers the region to the south of Cyprus, and its stronger element—the Shikmona eddy—is located immediately south of Cyprus. The Central Levantine Basin Current undulates in the region stretching from the southwest (the area of the data gap) towards Cyprus, then bifurcates southwest of the island. A branch flows north to enter the Antalya Basin, and the other branch, apparently carrying a larger flux flows east, then north along the Syrian coast to feed the meandering Asia Minor Current in the Cilician Basin. Most significantly, a coherent flow (the Asia Minor Current) meanders along the Anatolian coast, in the entire region from the Lattakia—Cilicia Basins to the Island of Rhodes. This pattern is radically different from the previous realizations of the circulation in which only a small fraction of the Central Levantine Basin Current was able to penetrate into the Cilician Basin through the eastern passage of Cyprus.

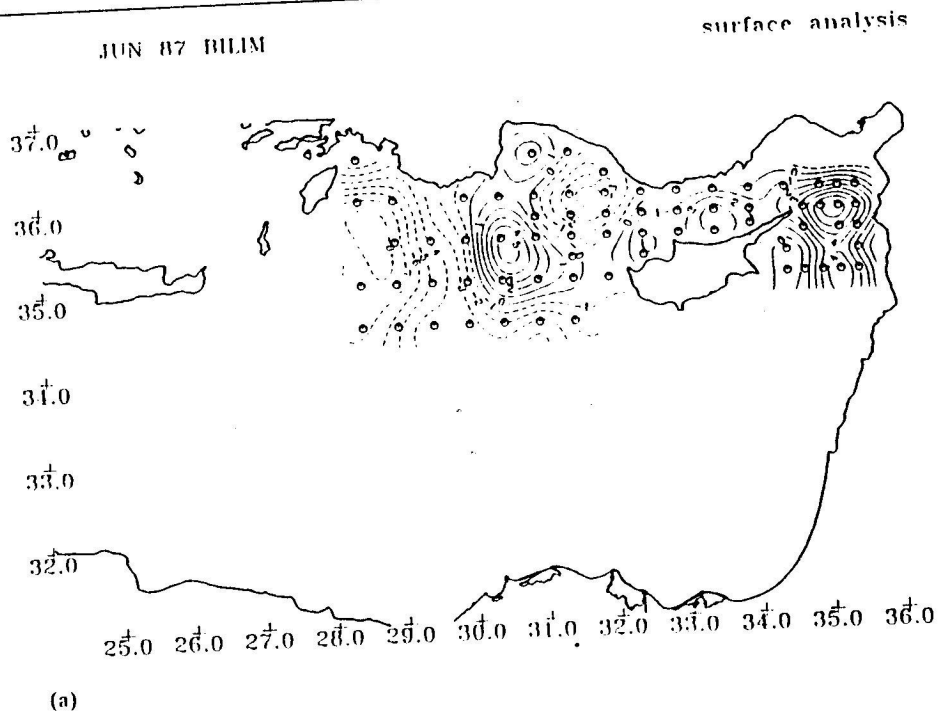

(a)

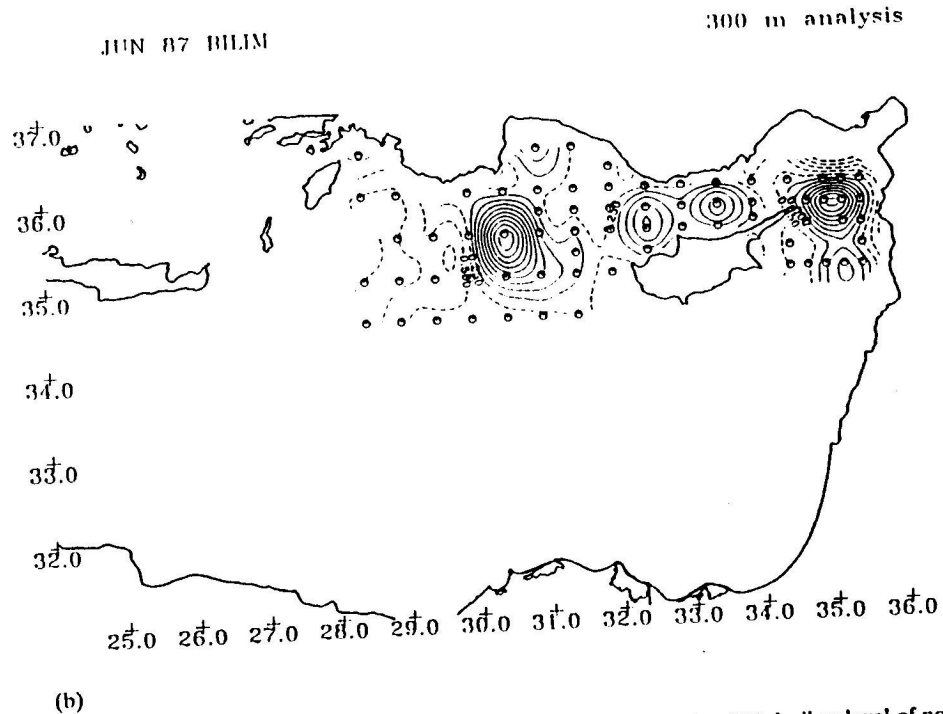

(b)

Fig. 4. (a) Surface and (b) 300 db dynamic height (in cm) referenced to 800 decibar level of no motion, June 1987.

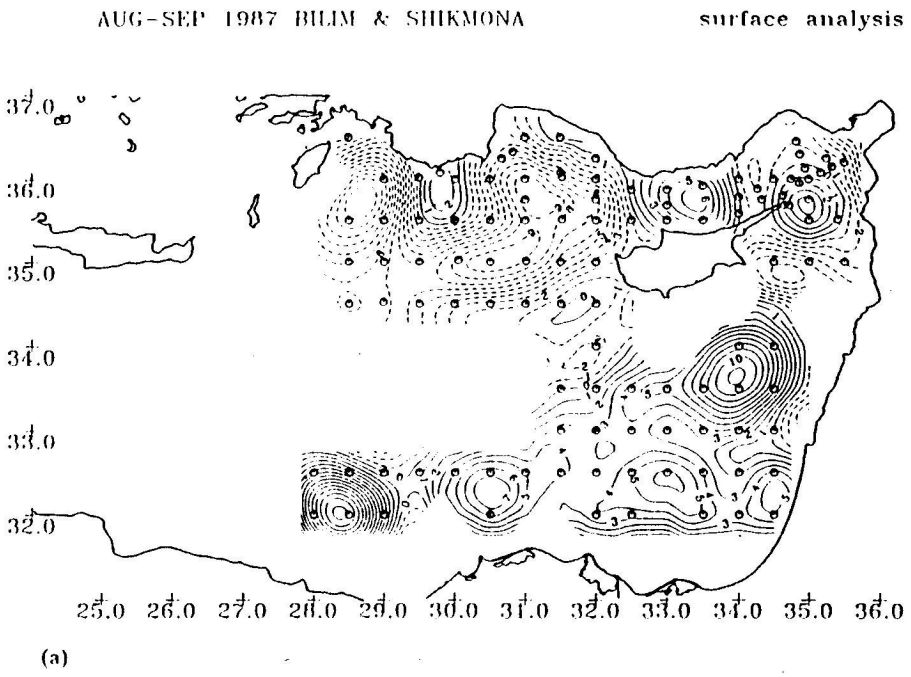

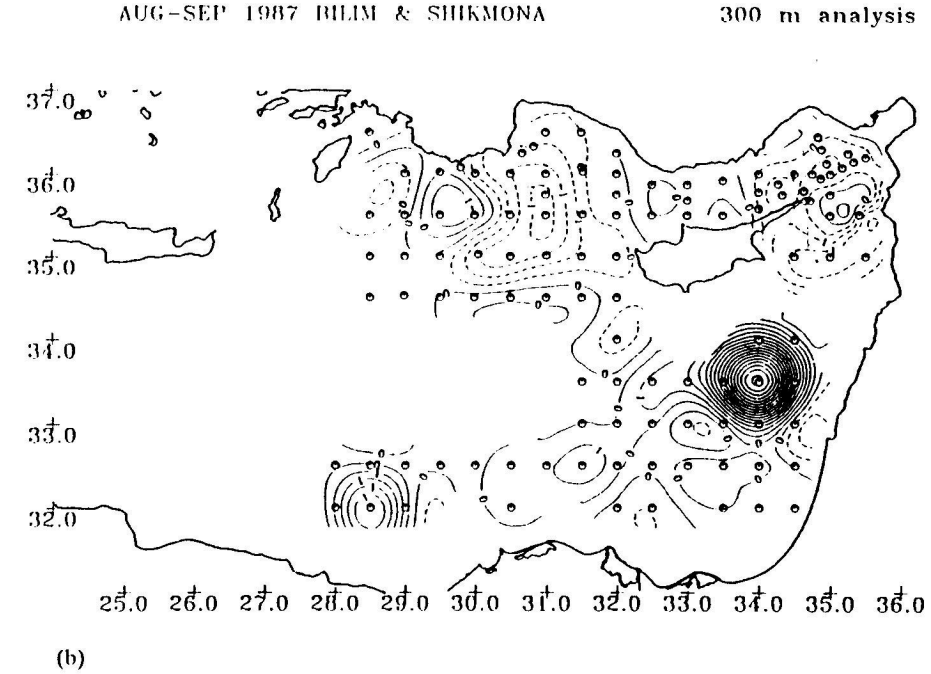

Fig. 5. (a) Surface and (b) 300 db dynamic height (in cm) referenced to 800 decibar level of no motion, August–September 1987.

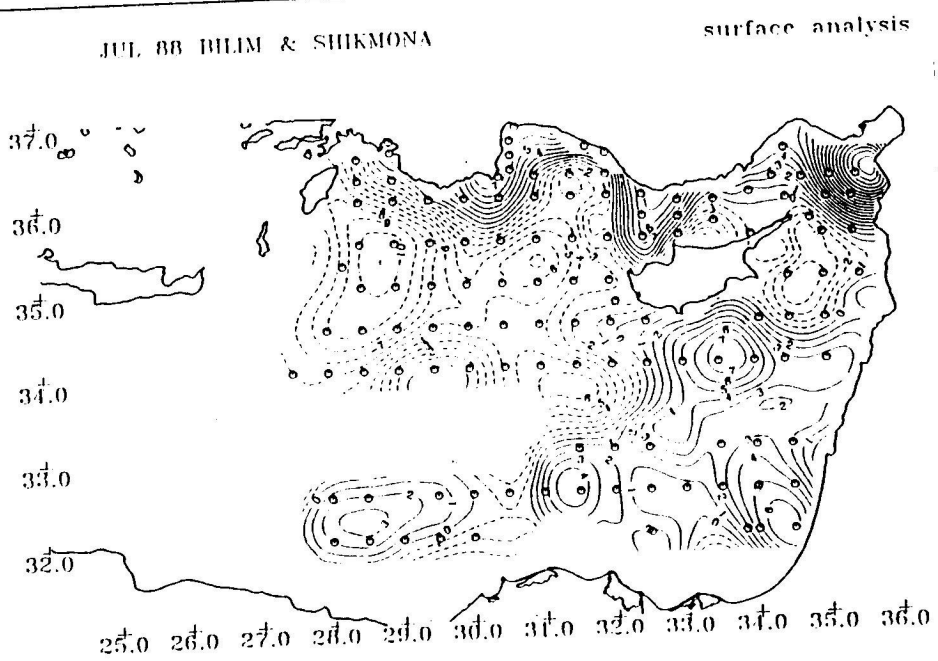

(a)

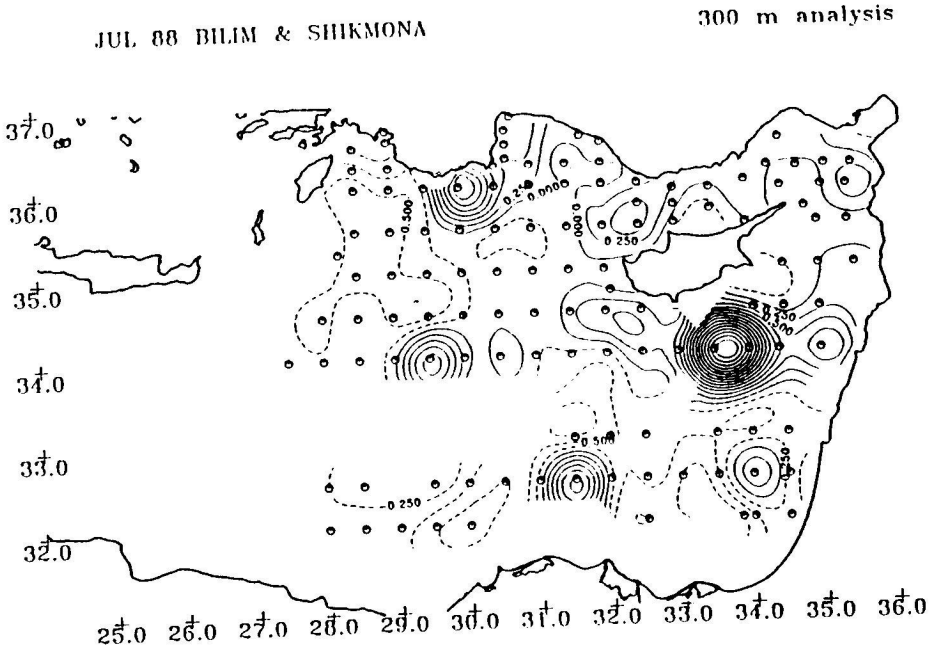

(b)

Fig. 6. (a) Surface and (b) 300 db dynamic height (in cm) referenced to 800 decibar level of no motion, July–August 1988.

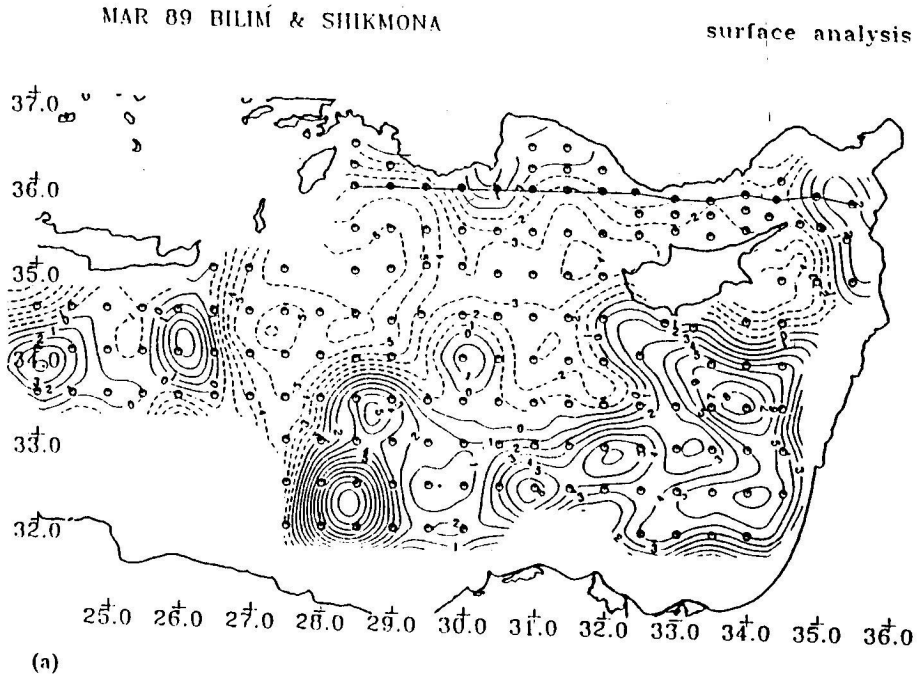

(a)

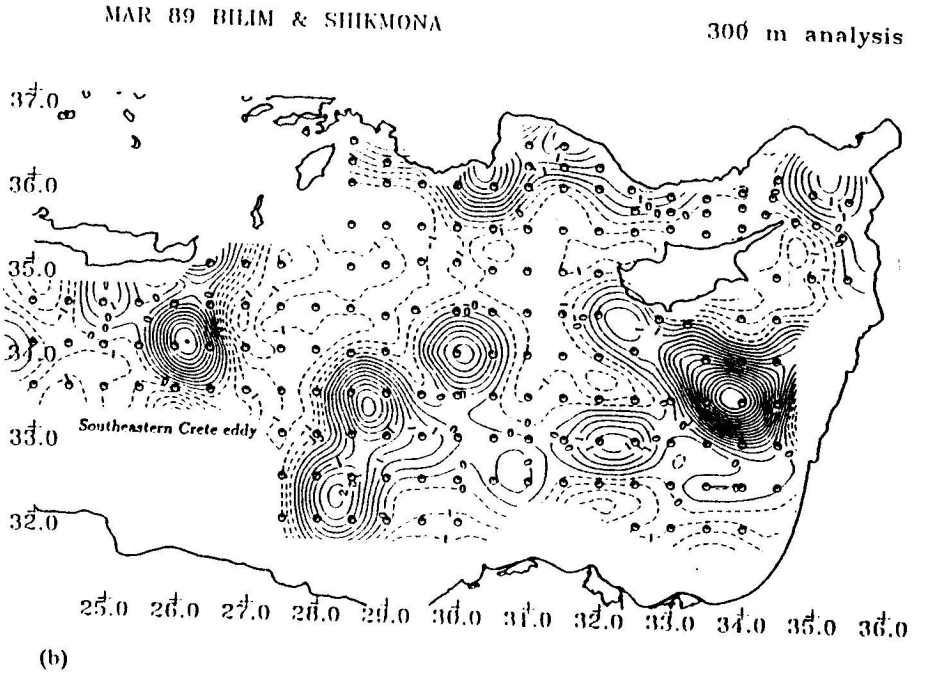

(b)

Fig. 7. (a) Surface and (b) 300 db dynamic height (in cm) referenced to 800 decibar level of no motion, March 1989.

The intermediate depth signatures [Fig. 6(b)] of coherent anticyclonic centers belong to the Anaximander eddy, the northern member of the Mersa Matruh Gyre, a southern member of the Shikmona complex off the Nile, and the Shikmona eddy south of Cyprus.

The circulation inferred from the partial survey in October 1988 is very similar to July–August 1988, indicating a persistent and meandering Asia Minor Current along the Cilician, Antalya and Rhodes Basins (Özsoy *et al.*, 1991). Similar to July 1988, the main part of the flow passes east of Cyprus to join with the meandering jet in the Cilician Basin.

The coverage of the entire Levantine Basin in the March 1989 (LBDS01) survey [Fig. 7(a)] allows a detailed analysis of the circulation. We observe a large area covered by the Rhodes Gyre, an intense anticyclonic eddy south of Crete, and numerous anticyclonic centers within the Mersa Matruh–Shikmona Gyre complexes. The circulation at 300 m depth shows coherent anticyclones in the same regions [Fig. 7(b)].

Because of a train of anticyclonic eddies in the south, the Central Levantine Basin Current cannot be observed in a continuous form in the Mersa Matruh region, though in the west, it appears as a southerly continuation of the Rhodes Gyre peripheral current, then flows along the northeastern boundary of the Mersa Matruh Gyre, and reorganizes itself into a coherent jet along the boundary of the Shikmona Gyre. The jet then flows towards the eastern Levantine shores and bifurcates there, with a branch circulating cyclonically around Cyprus and connecting into the Asia Minor Current, and the other branch completing a loop around the Shikmona complex. There is almost no flow entering into the Antalya Basin west of Cyprus. The northern Levantine circulation, with a continuous structure of the Asia Minor Current, is similar to the flow observed in July and October 1988, but appears weaker, as a result of thermocline erosion by outstanding winter convection events (Section 6). Similar changes of the Asia Minor Current were observed during the extreme event of deep and intermediate depth convection (Section 6.3) in winter 1991–1992 (Sur *et al.*, 1993).

The southeastern Cretan anticyclone observed in Fig. 7(a) and (b) seems to be a persistent feature, and the analyses of collective POEM05 data (Robinson *et al.*, 1991) show its existence in August–September 1987. Satellite remote sensing (Section 5) indicates an eddy in the same region in 1990, and in 1991 (not shown). Since the available data coverage is not continuous, we cannot tell if it is a persistent eddy. We only note that a similar feature was also observed in 1977 (La Violette, 1992).

In August 1990 (LBDS02), the northern Levantine circulation consists of a coherent flow of the Asia Minor Current along the Anatolian coast, with isolated anticyclonic regions trapped between the jet flow and the coast at the Anaximander and the Antalya Bay regions [Fig. 8(a)]. We can also identify the center of the Rhodes Gyre at the western part of the domain. At intermediate depths [Fig. 8(b)], we identify anticyclones at the Anaximander, Antalya Bay and Cilician Basin regions. The recurrent Antalya anticyclone has been restored in its preferred position about 4 years after its disappearance in late 1986.

It is interesting to note that the Antalya and Shikmona eddies change their position (by about 50–100 km) and intensity from one cruise to another. The deep core of the Antalya eddy (at 300 m) is observed at ~35° 30′N, 31° 30′E in October–November 1985 and June 1986, but shifts west in March–April 1986 and June 1987, and to the north when it is restored in August 1990. Similarly, the deep core of the Shikmona eddy observed at ~34°N, 34° 30′E in October–November 1985 shifts west in March–April 1986, then south in August–September 1987, returns north in July 1988, and back to the south in March

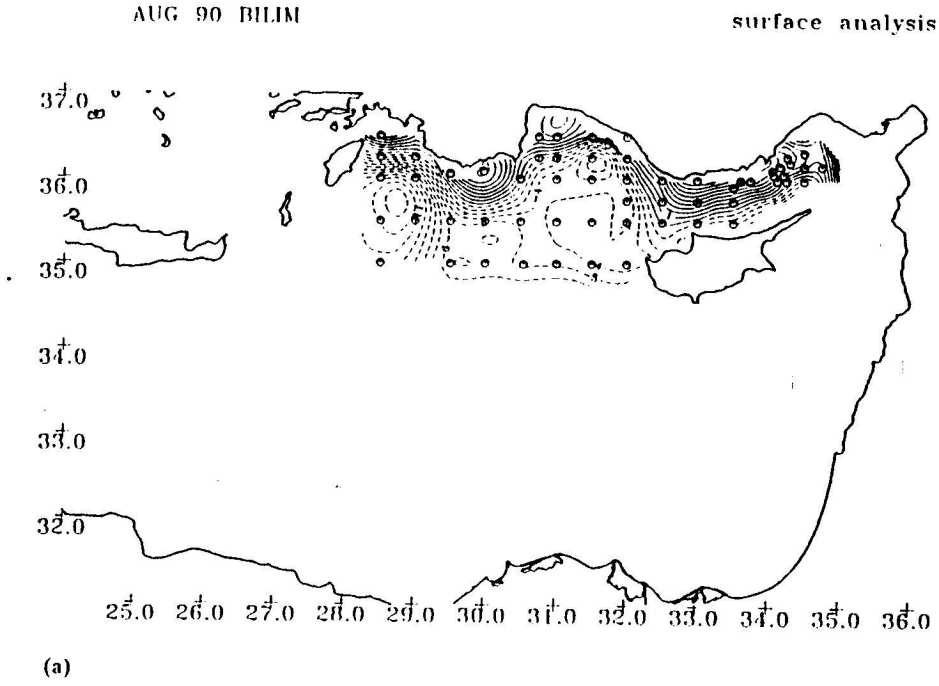

(a)

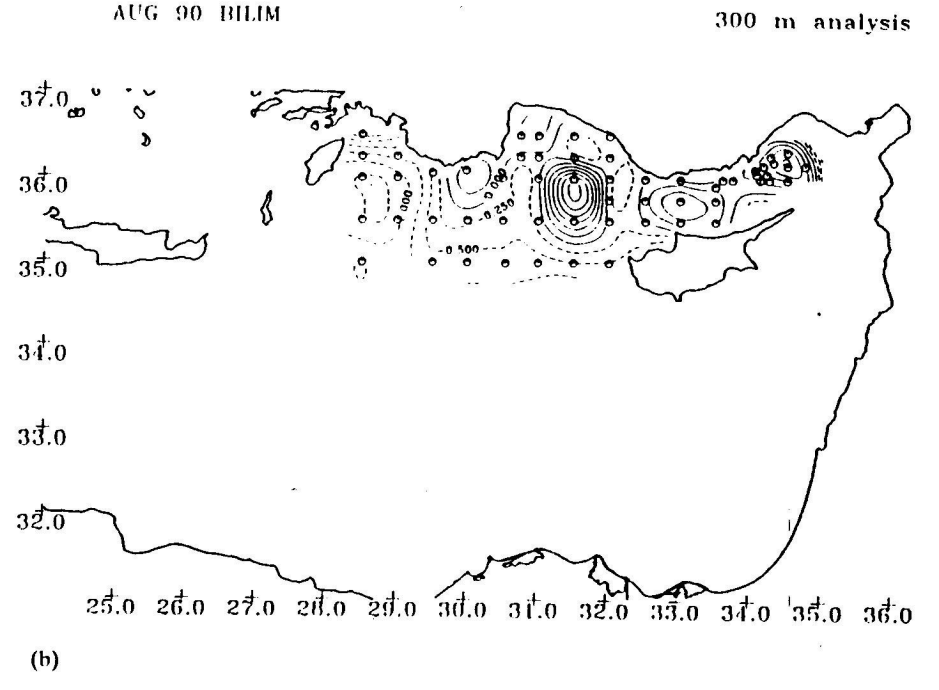

(b)

Fig. 8. (a) Surface and (b) 300 db dynamic height (in cm) referenced to 800 decibar level of no motion, August 1990.

1989. Further details based on other observations are given by BRENNER (1989, 1993) and BRENNER *et al.*, 1991).

It is also of interest to note the great vertical variations in some elements of the circulation. The greatest effects of such structure are observed in October–November 1985: note the horizontal shifts and intensity changes between the surface and 300 m circulation of the relative strengths of the Anaximanter–Antalya eddy pair, and of the eddies which are members of the Mersa Matruh and Shikmona Gyre complexes. The Antalya and Shikmona eddies are almost always relatively intensified at depth. The Antalya eddy in August 1990 did not have any anticyclonic signature at the surface, but the transient development of an anticyclonic feature is detected in satellite images (Section 5).

The development of the cyclonic Rhodes Gyre in the north, and anticyclonic Mersa Matruh and Shikmona Gyre complexes in the south of the Basin may have to do with the wind distributions, but the relationships are not well-established. OVCHINNIKOV (1966) suggested that the wind distribution was responsible for driving the North African Current and the gyres with opposite signs on its two sides. Indeed, estimates of MAY (1982), MALANOTTE-RIZZOLI and BERGAMASCO (1991) and PINARDI and NAVARRA (1992) indicate a reversal of the sign of wind stress curl from north to south, but the numerical models used by the latter authors fail to establish a simple north–south reversal in the polarities of the ocean gyres.

5. SURFACE FEATURES AND SATELLITE OBSERVATIONS

During the October–November 1985 (POEM01) surveys, surface features were sampled continuously along the ship track [Fig. 9(a)] in the northern Levantine (Özsoy *et al.*, 1986), yielding information on small scale surface variability. Continuous traces of temperature, salinity, σ_t density and phosphate [Fig. 9(b)] provide evidence for mesoscale

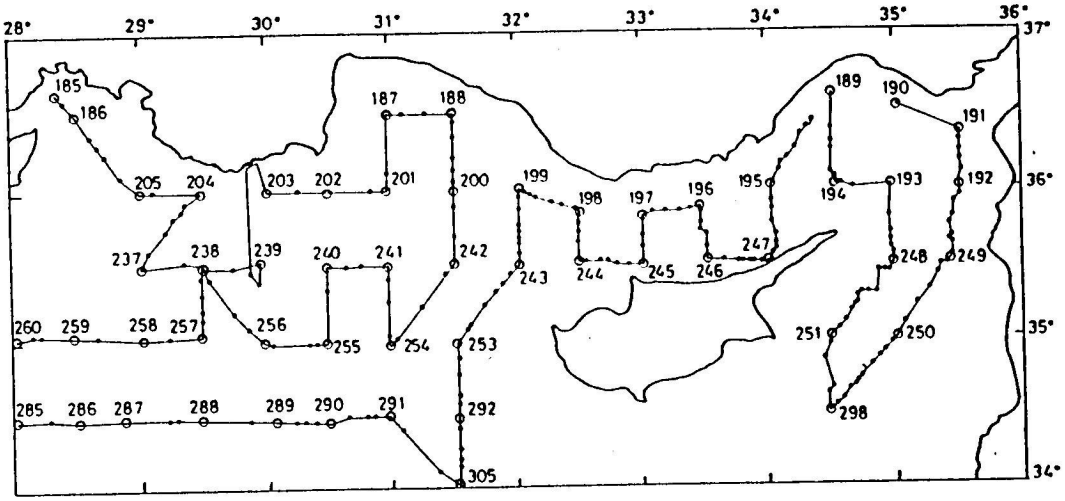

(a)

Fig. 9. (a) Stations and ship track of the R.V. *Bilim* in October 1985 (small dots are positions determined by satellite fixes); (b) Continuous traces of temperature, salinity, σ_t density and PO_4 along the ship track. Temperature fronts with gradients larger than 1°C km^{-1} are marked on the horizontal axis for temperature. Distribution of surface (c) temperature, and (d) salinity.

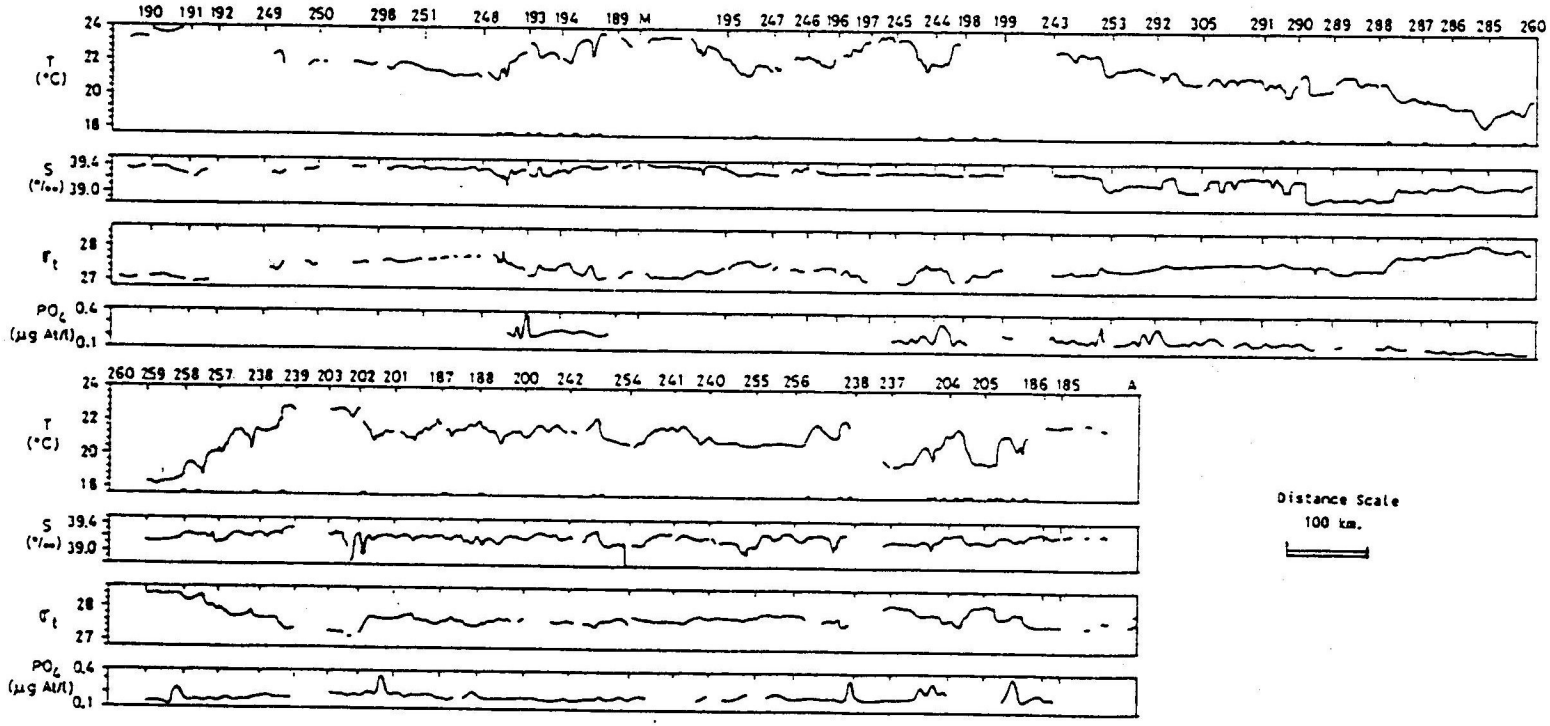

(b)

Fig. 9. (*Continued.*)

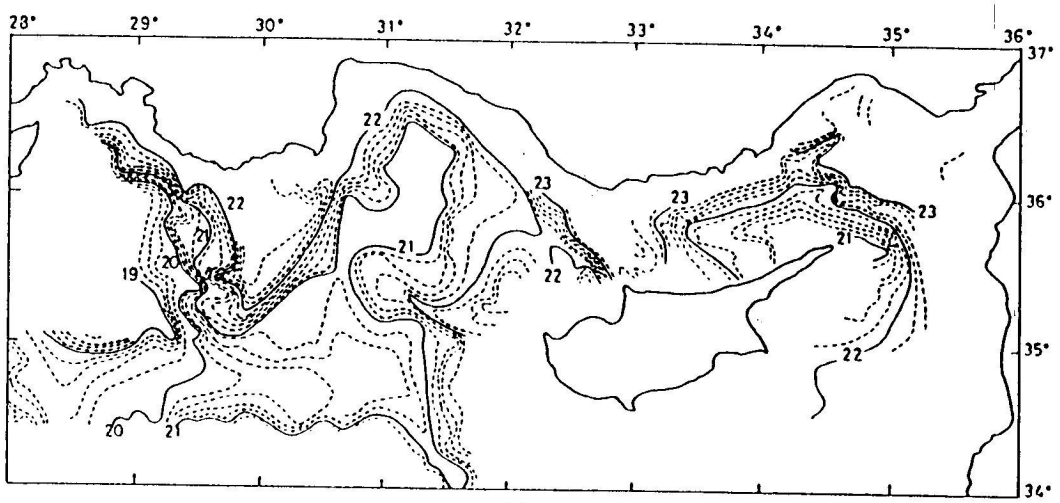

(c)

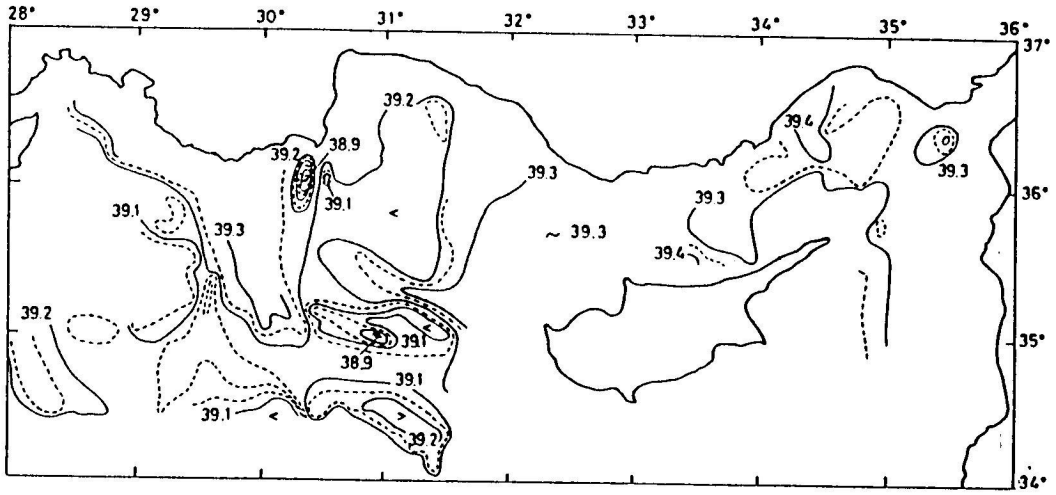

(d)

Fig. 9. (*Continued.*)

and sub-mesoscale activity, indicating temperature fronts with gradients exceeding 0.1°C km^{-1} in many areas. Salinity and phosphate concentration are uniform in most of the region, except near frontal regions where transient upward injections from subsurface waters could be found. The surface temperature and salinity are interpolated in Fig. 9(c) and (d). The mixed layer temperature is representative of the underlying circulation [Fig. 2(a)]. A sharp temperature front follows the coast and undulates around the Rhodes Gyre and the cyclonic area northeast of Cyprus, with large temperature differences (of up to 5°C) across it. The mixed layer salt balance appears largely determined by the surface buoyancy fluxes, since salinity is almost uniform in most of the region. The only significant changes occur in isolated spots influenced by the underlying Atlantic Water, as discussed in Section 6 (Fig. 12).

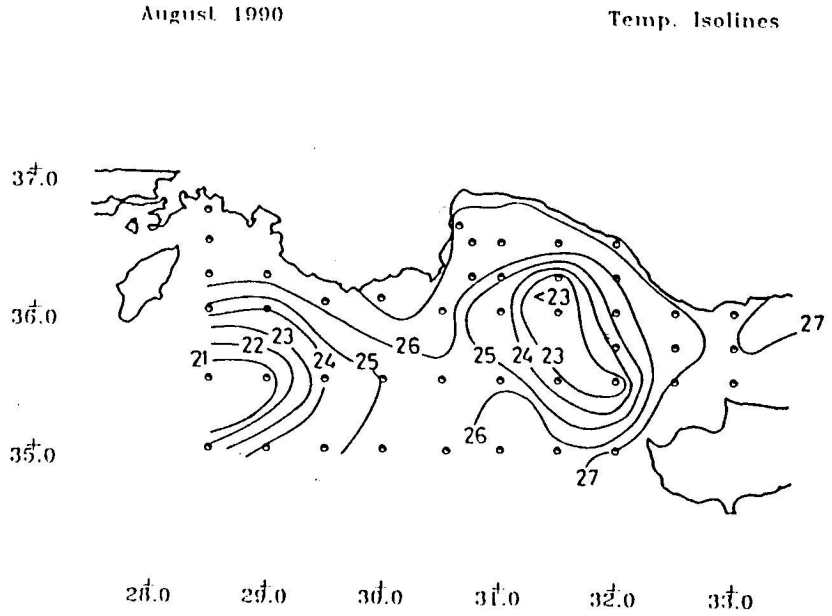

Fig. 10. Surface temperature distribution in northwestern Levantine Basin, August 1990.

The surface variability and relations to dynamical features are revealed by satellite data of August 1990. The temperature at 12 m depth (Fig. 10) indicates differences of up to 6°C between the coastal region and cold patches. The cold water patch in Antalya Bay occurs in the plateau-like extension of the Rhodes Gyre circulation [Fig. 8(a)], but at deeper levels it coincides with the center of the deep Antalya anticyclonic eddy [Fig. 8(b)]. A tendency for anticyclonic rotation is evident in the curvature of the Asia Minor Current as it exits the Cilician Basin [Fig. 8(a)]. Satellite data [Fig. 11(a)–(c)] available in the following period show the development of an anticyclonic feature from an instability of the Asia Minor Current.

Cold surface waters of the Rhodes Gyre and its meso-scale features are illustrated in the first image of August 21 1990 [Fig. 11(a)], where a cold filament extends from the Rhodes Gyre region into Antalya Bay. The warm coastal waters of the Asia Minor Current are also easily identified, becoming wider near the Anaximander anticyclone. Another region where the coastal jet becomes wider is near the eastern part of Antalya Basin where a warm water filament from the warm coastal region extends to the southwest, opposite to the direction of the cold water filament. On the August 29 image [Fig. 11(b)] the warm water filament spirals in an anticlockwise sense and engulfs a cold water extension of the Rhodes Gyre in Antalya Bay. On August 30 [Fig. 11(c)], features of the spiral filament and the cold water at its center are more visible.

A number of other dynamical features are evident in the clear image of Fig. 11(b). The Rhodes Gyre displays undulations on its periphery and along a filament connecting it to the Island of Karpathos. The two axisymmetrical eddies of ~100–150 km diameter southeast of Crete and at the middle of the Basin have been detected in earlier CTD surveys. The southeast Cretan eddy was present in August–September 1987 (Robinson *et*

al., 1991a) and March 1989 [Fig. 7(a) and (b)]. The other anticyclonic eddy, which appears as a northerly member of the Mersa Matruh complex, was detected in coherent forms in July–August 1988 (Fig. 6(a) and (b)] and March 1989 [Fig. 7(a) and (b)]. Other eddies of similar size are also evident in the southern part of the Cretan Passage.

Another interesting feature in Fig. 11(b) and (c) is the cold water filament extending first southeast then east from the southwestern corner of the Island of Cyprus. This cold water filament appears to be the result of upwelling, possibly driven by westerly winds, and consistently observed in other satellite images of summer 1990. Similar upwelling features south of Crete are reported by La Violette (1992).

6. TRANSPORT, CONSERVATION AND PRODUCTION OF WATER MASSES

6.1. *AW and LIW in filaments and coherent eddies*

Intimate relationships exist between the property distributions and the upper ocean circulation, exemplified through salinity distributions. The near surface contours with salinities of 38.9 or less are used to identify the AW, and salinities of 39.0 and greater at intermediate depths are used to characterize the LIW, despite difficulties in assigning any absolute limits to either water mass (Özsoy *et al.*, 1989).

The AW enters the southern Levantine Basin through the Cretan Passage, becomes pooled in the large southern anticyclonic gyres, and by advection and entrainment reaches the northern Levantine region in the form of filaments below the mixed layer, encircling the Rhodes Gyre and other eddies in the region (Özsoy *et al.*, 1989, 1991). The AW pool in the southern Levantine and the penetration of its filaments into the northern Levantine can be observed in Fig. 12. Comparison with Fig. 2(a) indicates a pattern of advection by the existing circulation. [A filament penetrating north along 31° 30′E is shown in Figs 8 and 12(b) of Özsoy *et al.* (1989).] The low salinity surface waters near 35°N 31°E in Fig. 9(d) could originate from a transient frontal upwelling of this subsurface filament. As far as they can be resolved by the station network, such filaments can be characterized with widths of 30–50 km and length scales of 100–200 km.

In October–November 1985, small pockets of AW filaments in the northern Levantine are sandwiched between the high salinity LIW and the mixed layer [Fig. 13(a)]. The isohalines rise in the west due to the Rhodes Gyre, and maximum salinity LIW is stored in the core of the intense Antalya anticyclonic eddy. Similar features are observed later in June 1986 [Fig. 13(b)].

In February 1987, when significant changes occurred in the circulation (Section 4), anticyclonic eddies arriving in the Lattakia Basin carried with them AW, from the surface to a depth of 200 m [Fig. 13(c)].

In the following June 1987, a massive invasion of the Northern Levantine by AW [Fig. 13(d)] covered the Lattakia, Cilicia and Antalya Basins and penetrated into the core of an anticyclonic eddy south of Antalya Bay. It is significant that the structure of the Antalya eddy has been completely renewed by AW entrained into its core and the salinity and total volume of the underlying LIW in its core has decreased [compare Fig. 13(b) and (d)]. Neither the Anaximander and Antalya eddies at earlier times seemed to carry AW in their cores, and a merger of the former eddies (Section 4) would still be insufficient to explain its water mass structure. The AW entrained in the new eddy could have come from the surroundings, or from an earlier interaction with a third anticyclonic eddy transporting

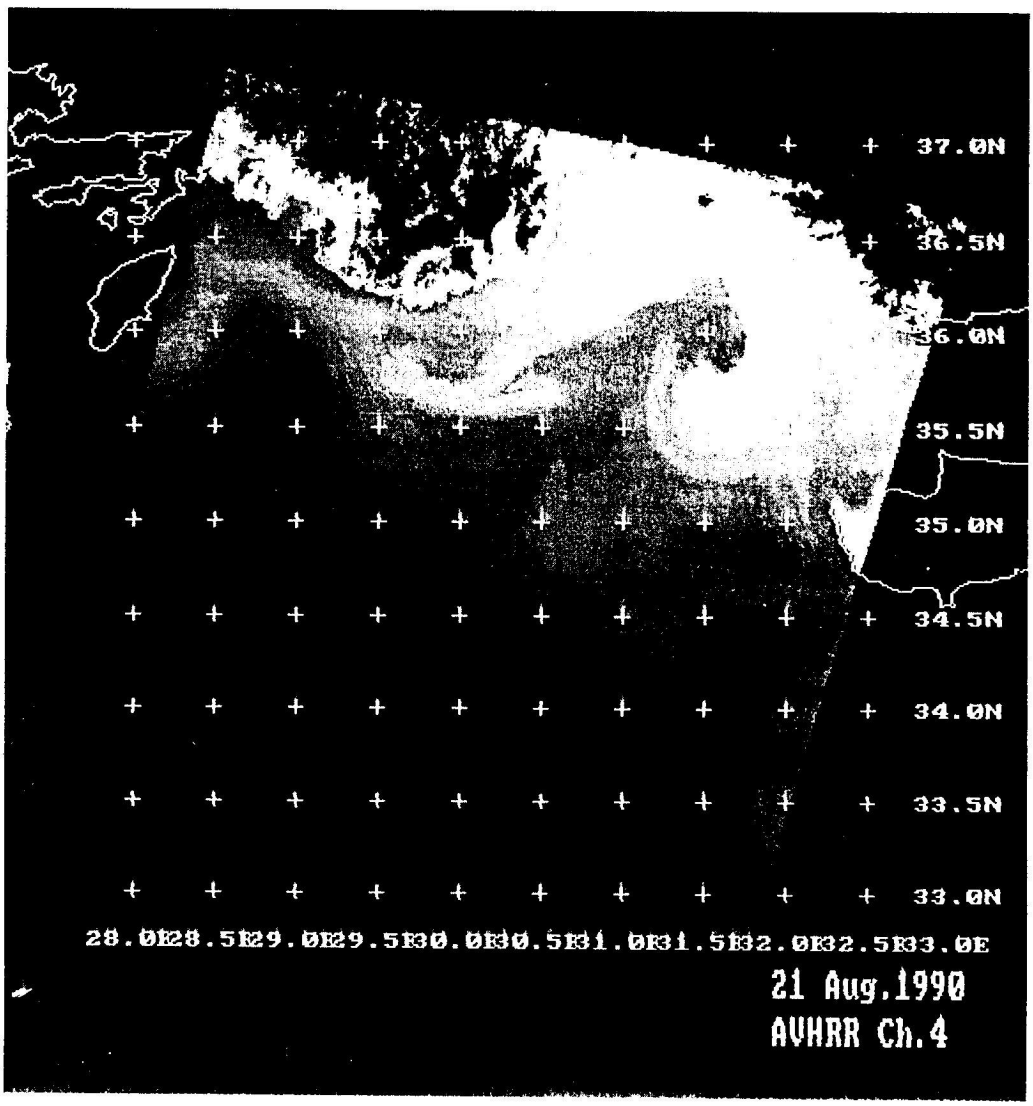

(a)

Fig. 11. AVHRR satellite images of the Levantine Basin: (a) 21 August, 1990, NOAA-11, orbit:20386; (b) 29 August, 1990, NOAA-10, orbit:20500; (c) 30 August, 1990, NOAA-10, orbit:20514.

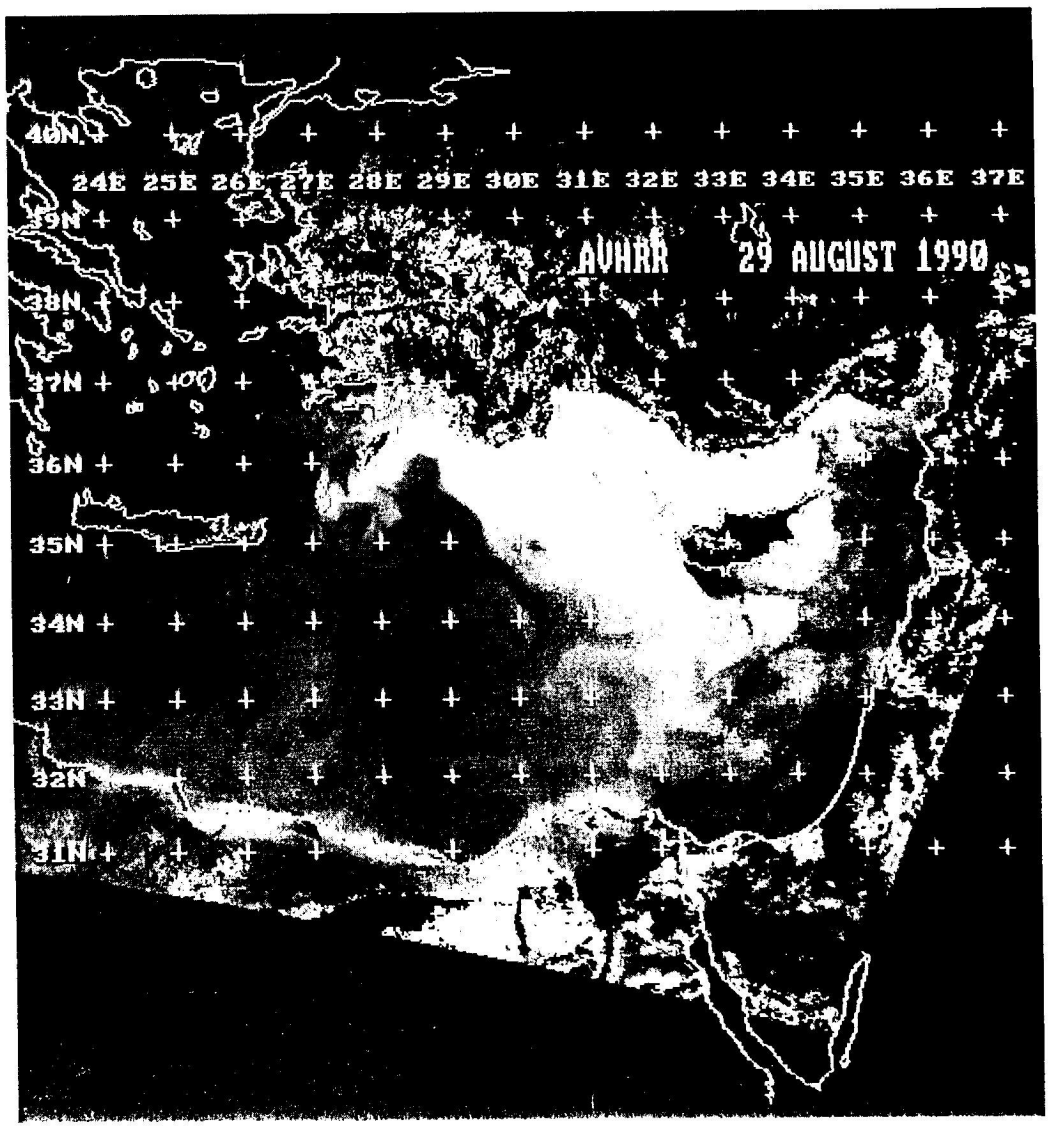

(b)

Fig. 11. (*Continued.*)

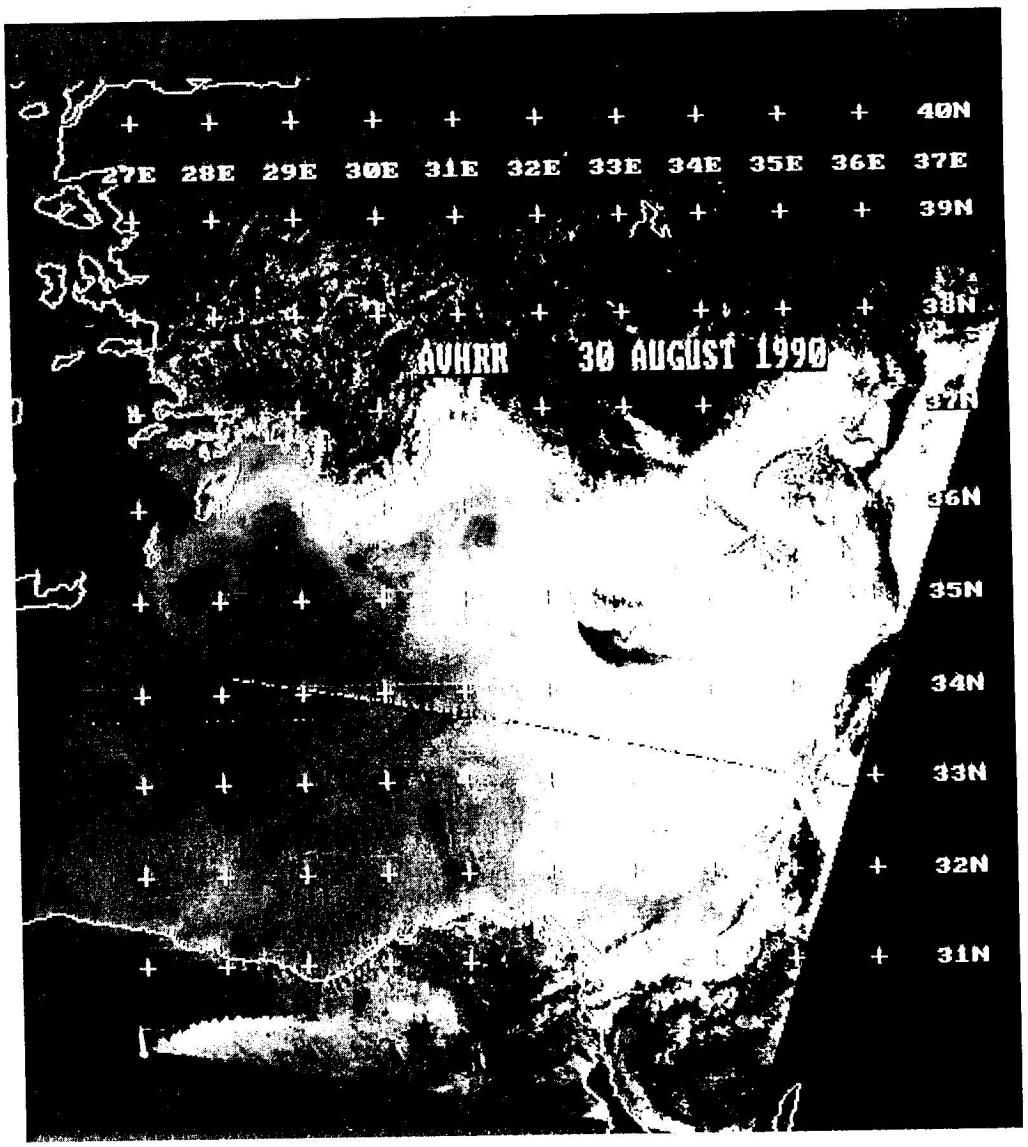

(c)

Fig. 11. (*Continued.*)

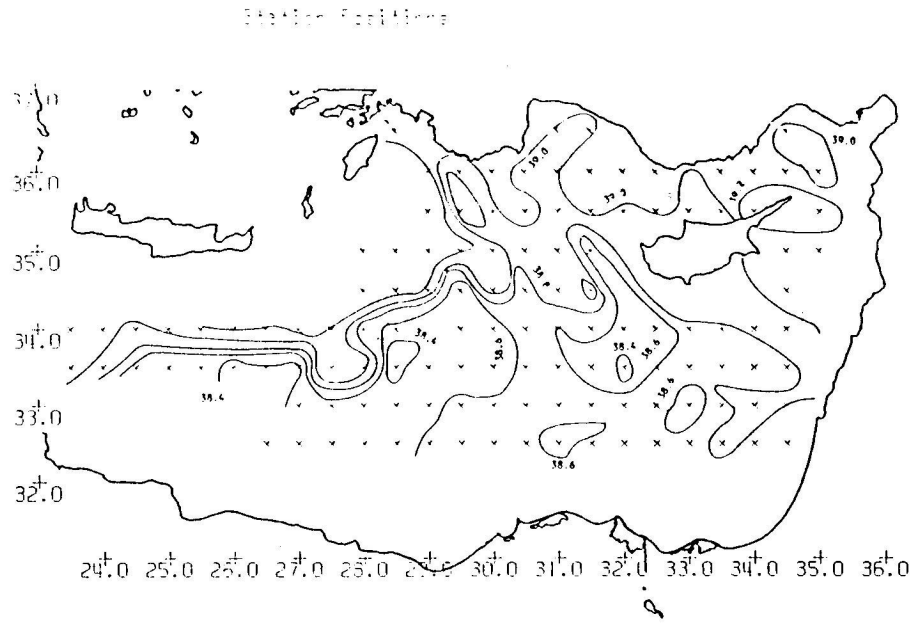

Fig. 12. Salinity on the density surface of $\sigma_t = 28.0$, corresponding to the Atlantic Water (AW) core below the mixed layer, October–November 1986.

AW across the Cilician Basin, i.e. similar to that shown in Fig. 13(c). Merging eddies could exchange water particles between them, as well as with the surrounding waters, via intrusions and filaments. PAVIA and CUSHMAN-ROISIN (1990) were able to show almost complete substitution of the water particles in one of the interacting eddies with those of the other.

In August–September 1987, the thin filaments of AW below the mixed layer in the Antalya and Cilician Basins (ÖZSOY *et al.*, 1991) were significantly reduced in comparison to June 1987. The Shikmona eddy, embodying a uniform mass of LIW in earlier surveys, was penetrated by AW (BRENNER *et al.*, 1991). (A similar invasion of AW also occurred during winter 1989–90, BRENNER, 1993.)

All of the above observations indicate that the year 1987 was a period of rapid changes in the circulation and water mass structures of the Levantine Basin. The following data sets in July and October 1988 (ÖZSOY *et al.*, 1991), and a basin-wide survey in March 1989 (reviewed separately in the next Section) showed a continuing trend in the Northern Levantine of very little AW, but a continued abundance of LIW. The August 1990 data show a reformed Antalya anticyclone, with a high salinity LIW core [Fig. 13(e)], similar to that observed prior to 1986. A single transect of stations covered in November 1990 [Fig. 13(f)] indicates the continued presence of the Antalya anticyclone till late 1990.

6.2. *Convection and LIW production during the winters of* 1988–1989 *and* 1990–1991

Extensive LIW formation in the Northern Levantine basin was discovered during the March 1989 observations, whose distinguishing feature, compared to earlier observations,

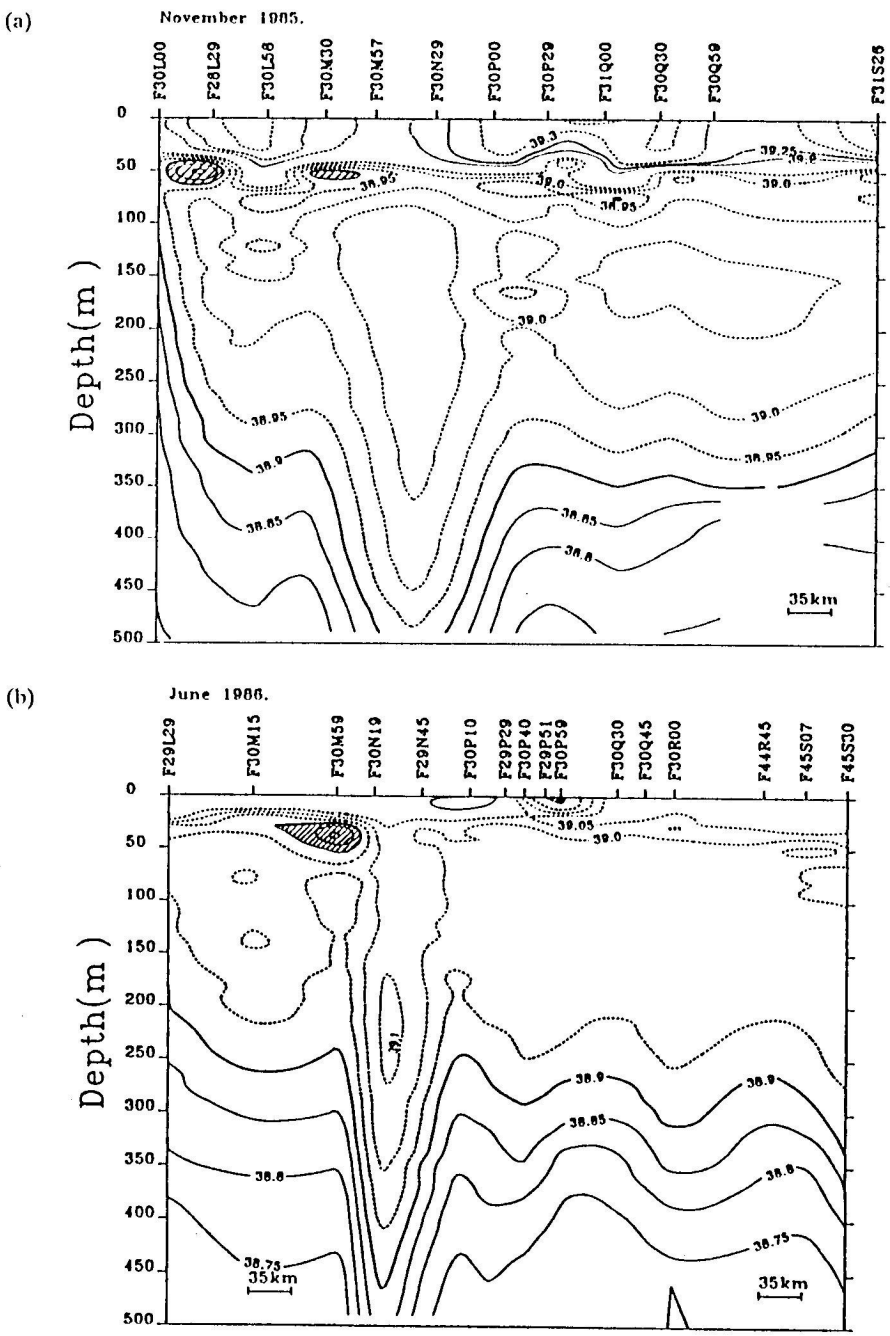

Fig. 13. West–east section of salinity in the northern Levantine in (a) October–November 1985, (b) June 1986, (c) February 1987, (d) June 1987, (e) August 1990, (f) November 1990 (see Fig. 2 for letter coding used in station labels. The position of a station is indicated by a three character code for latitude, composed of the character code and nearest division of minutes, followed by another three characters for longitude: e.g. Sta. F30N30 corresponds to 35° 30′N, 31° 30′E).

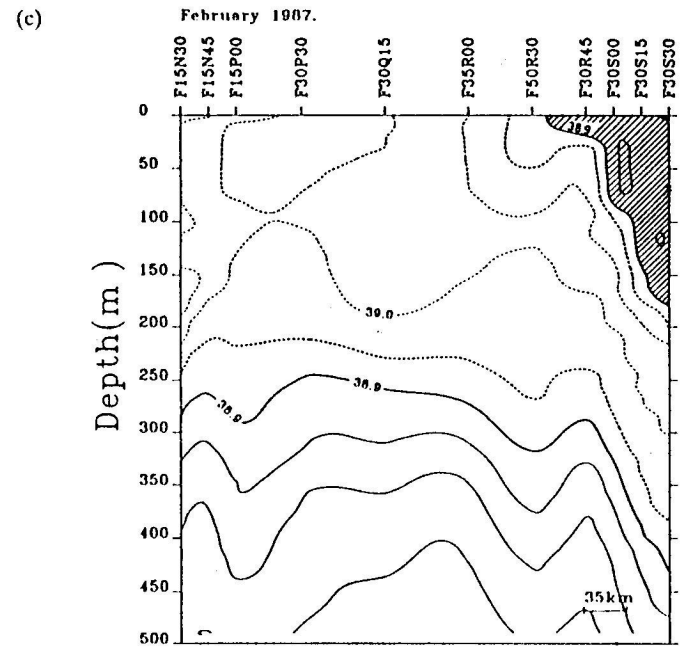

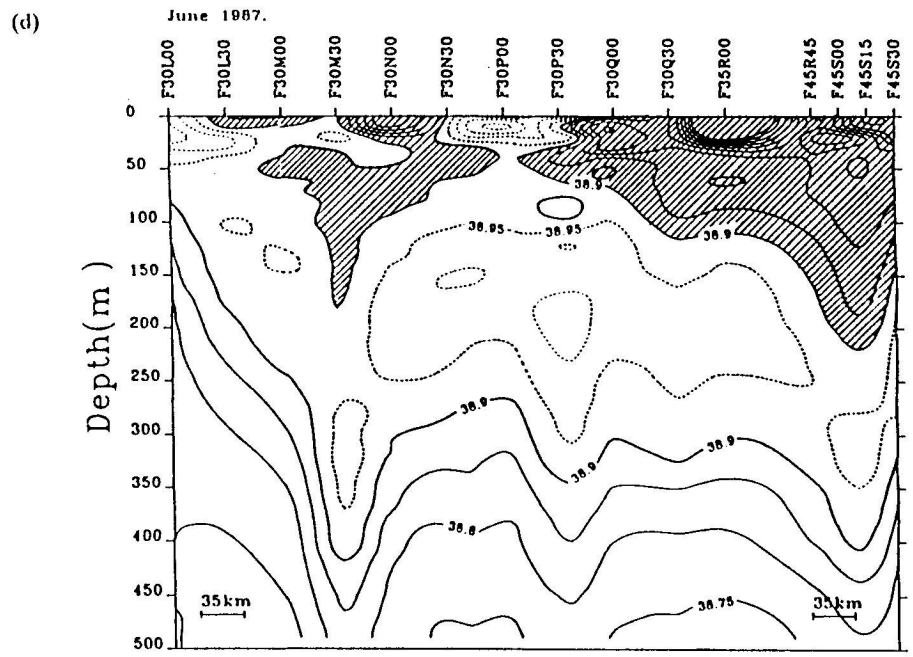

Fig. 13. (*Continued.*)

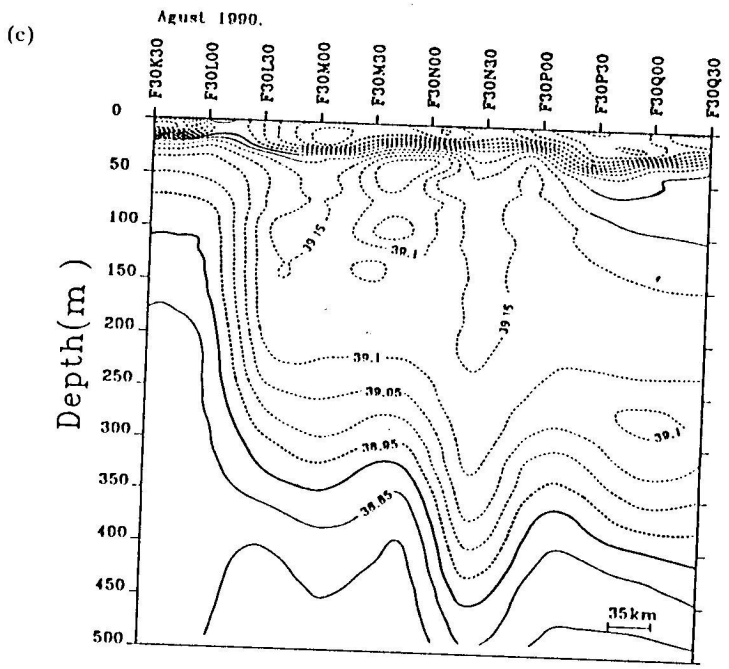

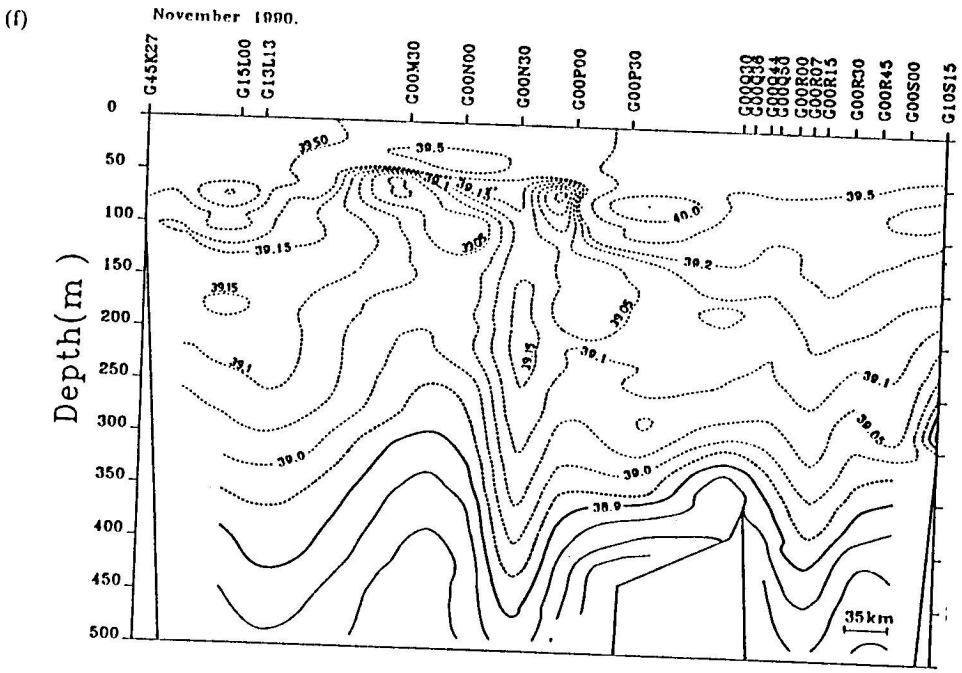

Fig. 13. (*Continued.*)

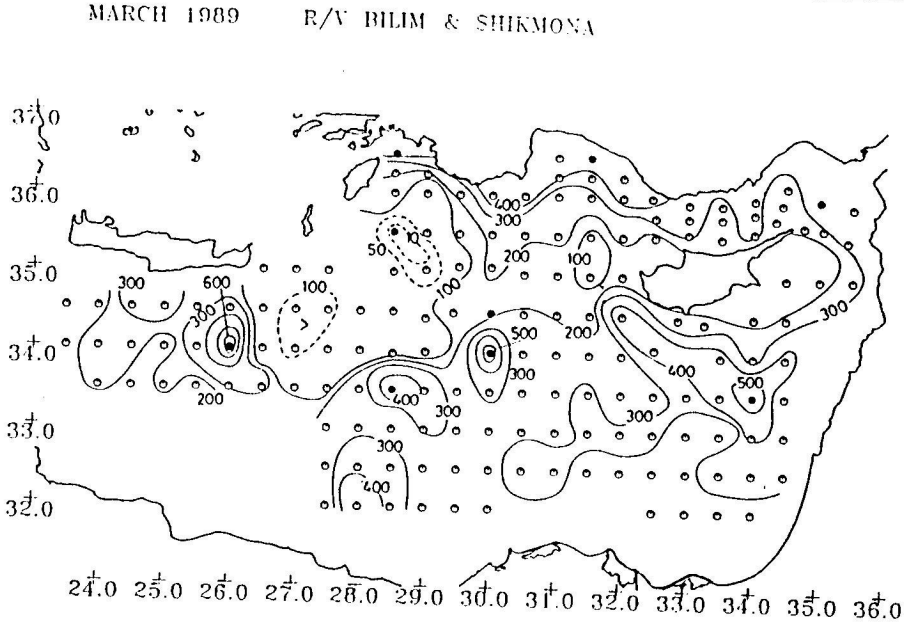

Fig. 14. The depth of the 15°C isotherm in the Levantine Basin, March 1989. Solid markers are the positions of stations whose data are presented in Fig. 15(a)–(i).

was a region of mixing extending from the surface to depths of several hundreds of meters in many areas, and anomalous deep features in the temperature–salinity profiles, evidently resulting from wind-mixing and convective overturning.

The basin-wide distribution of the depth of 15°C, an approximate indicator of the base of the mixing layer (Fig. 14), indicates deepening of the isotherm to more than 500 m at the centers of some anticyclonic eddies [Fig. 7(a) and (b)], and along the Anatolian coast, and in contrast, becoming as shallow as 10 m at the center of the Rhodes Gyre. Since Fig. 14 can be misleading when the deepening is associated with conservative eddy motions rather than mixing, we also review in Fig. 15(a)–(i) selected stations to illustrate mixing effects.

Along the Anatolian coast [Fig. 15(a)–(c), stations marked in Fig. 14], properties were almost uniform in the upper 300–400 m and covered the entire coast [Fig. 16(a) and (b)]. The mixed layer extended to 300 m at the center of the Shikmona eddy [Fig. 15(d)] and to 300–400 m at the centers of the two Mersa Matruh eddies [Figs 15(e) and (g)]. North of the Mersa Matruh eddies, some deep structures were found at the frontal region adjoining the Rhodes Gyre [Fig. 15(f)]. Typical LIW values of θ = 15–16°C and S = 39.0–39.1 were found in the cores of eddies and along the Asia Minor Current. Outside the domain of influence of the above features, the mixed layer was either shallower or was not well-defined. For example, the southernmost member of the Mersa Matruh eddies [Figs 7(a) and (b) and 14] contained AW near the surface, without any evidence of mixing (not shown). The southeast Cretan eddy [Fig. 15(h)] had a deep structure of relatively warm, saline water throughout its depth, with a mixed layer of 200 m depth. It is interesting to note that the center of the Rhodes Gyre had almost uniform density throughout the water column, excluding the small gradient in the upper 100 m, that evidently was not overcome

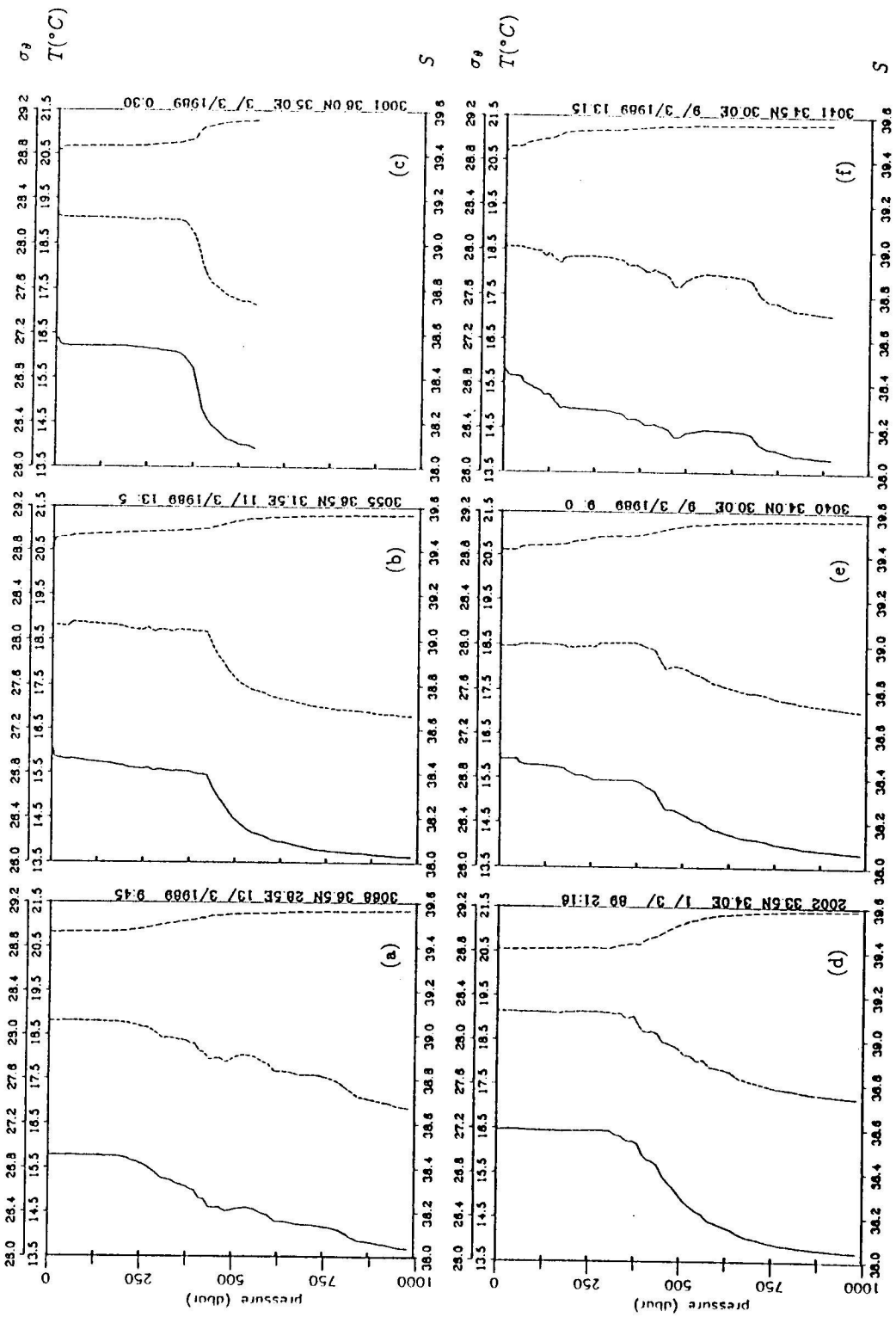
σθ
T(°C)
S
(a)
(b)
(c)
(d)
(e)
(f)
pressure (dbar)
0
250
500
750
1000

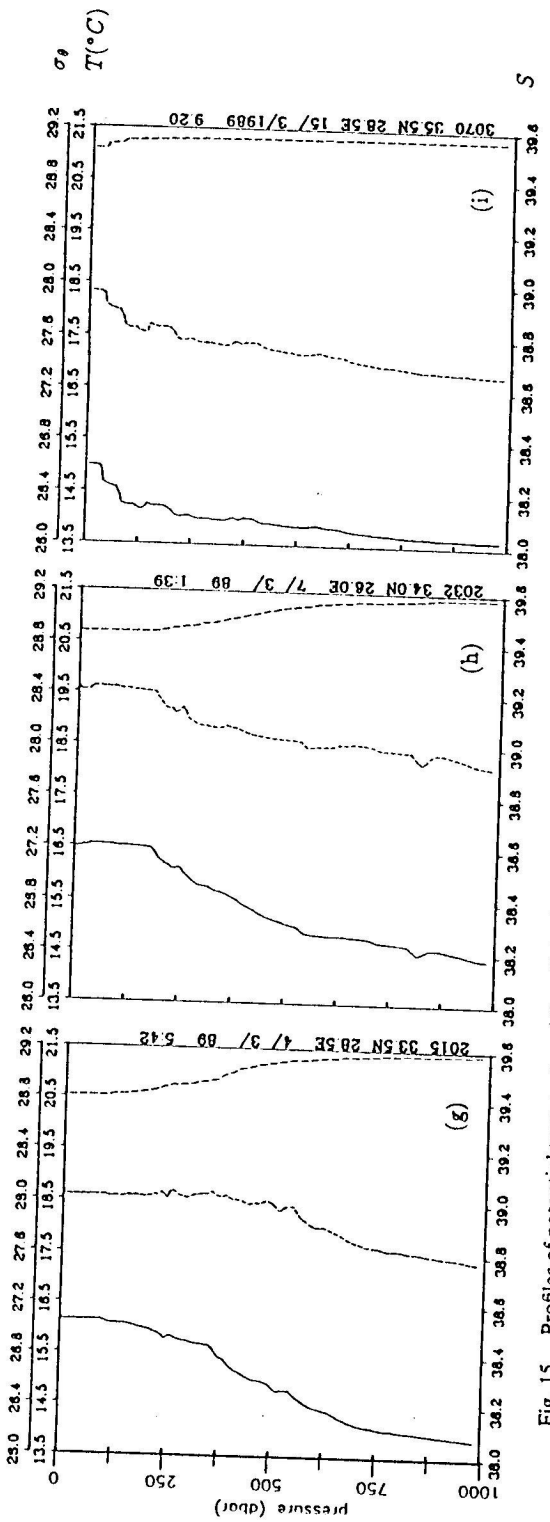

Fig. 15. Profiles of potential temperature (θ), salinity (S) and density (σ_θ) at selected stations, March 1989. (a) 36°30′N, 28°30′E, (b) 36°30′N 31°30′E, (c) 36°N 35°E, (d) 33°30′N 34°E, (e) 34°N 30°E, (f) 34°30′N 30°E, (g) 33°30′N 29°30′E, (h) 34°N 26°E, (i) 35°30′N 28°30′E.

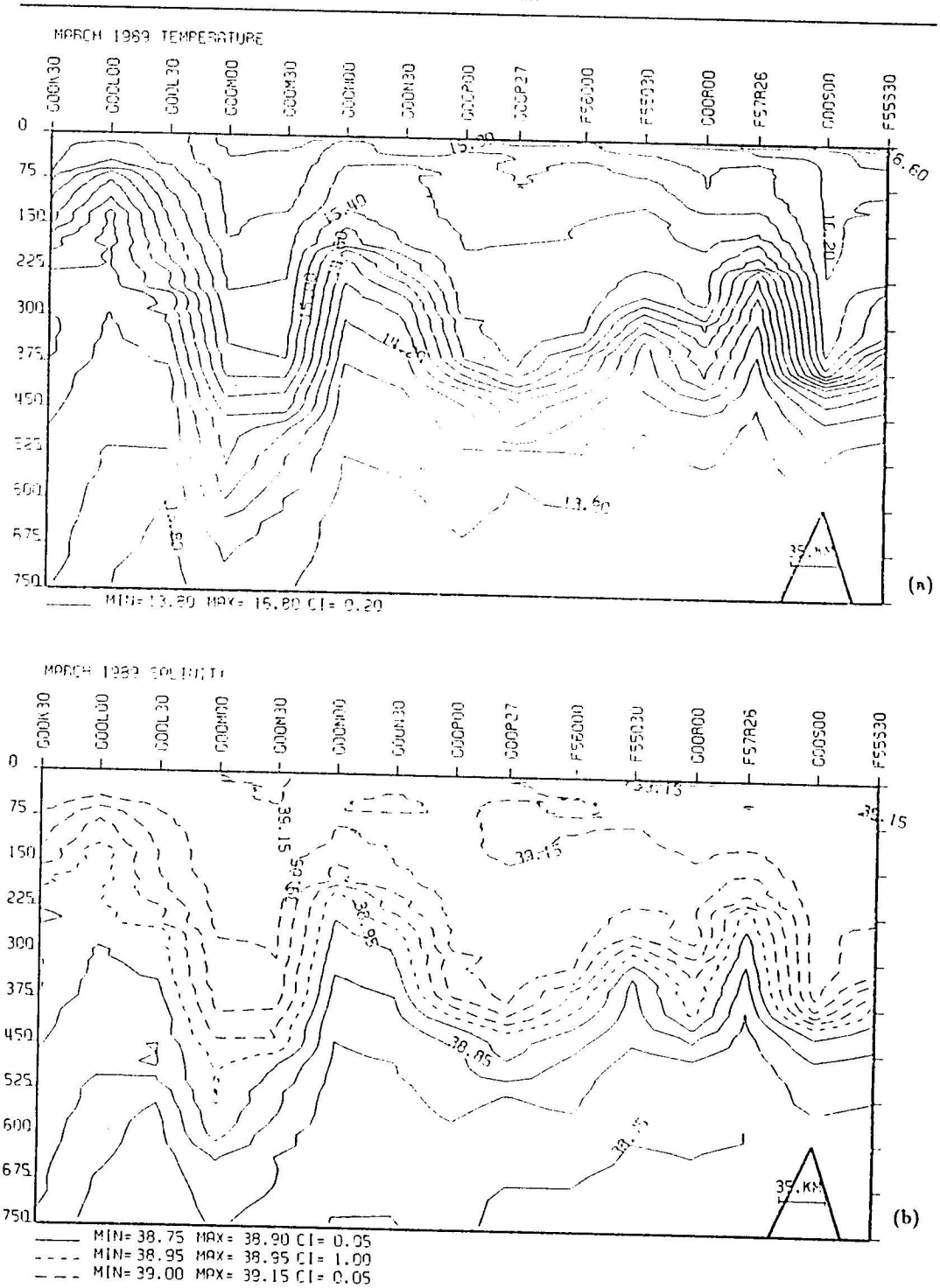

Fig. 16. (a) Temperature and (b) salinity east–west sections in the northern Levantine Basin, March 1989.

by the cooling and wind-mixing leading to convection elsewhere. A further erosion of its cap could have resulted in deep convection to depths ≥1000 m (Section 6.3), but at least in this case it stopped short of overturning.

Convective overturning also was detected in a limited survey in March 1991 (Section 6.4), when LIW with even higher salinity than in 1989 was formed in a mixed layer reaching depths of 400–500 m along the Anatolian coast.

Local production of LIW in anticyclonic eddies by convective overturning has been demonstrated in the case of the Shikmona Gyre (Brenner *et al.*, 1991) under the effects of surface buoyancy fluxes. Similar one-dimensional formulations were found appropriate to study the evolution of anticyclonic eddies (e.g. Schmitt and Olson, 1985; Dewar, 1986). Aided by a pool of warm water with low static stability above a deep thermocline, anticyclonic eddies can be subjected to increased buoyancy fluxes and to efficient mixing under winter atmospheric conditions.

Feliks (1991) incorporated stability dependent mixing, the effects of coasts and the recurrent forcing by winter storms into a two-dimensional model of the Levantine Basin, and was able to generate intermediate depth mixing and LIW formation in the entire region, with increased depth and uniformity along the coast.

It seems that either of the local production hypotheses in the above models are consistent with the observations. However, three-dimensional and isopycnal processes can exist at the same time. Packets of anomalous saline water have consistently been found on the periphery of the Rhodes Gyre (e.g. Özsoy *et al.*, 1989). Features similar to those in Fig. 15(f) were common during March 1989, and interleaving of waters with different properties were evident in many regions.

6.3. *Intermediate and deep convection during the winter of* 1991–1992

A set of unique observations in March 1992 (Sur *et al.*, 1992) have recently indicated intense mixing in the entire northern Levantine Basin, leading to simultaneous formation of LIW and Deep Water (DW), observed for the first time in the region. At the center of the Rhodes Gyre [Fig. 17(a)], uniform Deep Water properties ($\theta \simeq 13.7$, $S \simeq 38.8$) extended to depths of ≥1000 m. In the adjoining waters [Fig. 17(b)], a deep mixing layer (300–700 m) with uniform LIW properties ($\theta \simeq 15.2$–15.5, $S \simeq 39.1$–39.2) was found. The only previous occurrence of DW formation in the region was observed in 1987 by Gertman *et al.* (1990), in which case the uniform values observed at the center of the Rhodes Gyre ($\theta \simeq 14.0$, $S \simeq 38.9$) extended to depths of 500–600 m. Our observations indicate a recurrence with deeper, more efficient mixing 5 years later.

6.4. *Potential temperature–salinity relationships*

The water mass and mixing characteristics can be traced through the θ–S relationships (Figs 18–20), grouped together according to periods of apparent similarities. The first period [Fig. 18(a)–(e)] is from October 1985 to June 1987. Similar features are observed in September 1987, but this data set is excluded due to salinity drifts in the R.V. *Bilim* data. Figure 18(a) and (b), covering the entire Basin, is biased by an abundance of AW in the southern Levantine, relative to the other data sets covering only the north. A similar bias is also present between cruises of different areal coverage.

by the cooling and wind-mixing leading to convection elsewhere. A further erosion of its cap could have resulted in deep convection to depths ≥1000 m (Section 6.3), but at least in this case it stopped short of overturning.

Convective overturning also was detected in a limited survey in March 1991 (Section 6.4), when LIW with even higher salinity than in 1989 was formed in a mixed layer reaching depths of 400–500 m along the Anatolian coast.

Local production of LIW in anticyclonic eddies by convective overturning has been demonstrated in the case of the Shikmona Gyre (Brenner *et al.*, 1991) under the effects of surface buoyancy fluxes. Similar one-dimensional formulations were found appropriate to study the evolution of anticyclonic eddies (e.g. Schmitt and Olson, 1985; Dewar, 1986). Aided by a pool of warm water with low static stability above a deep thermocline, anticyclonic eddies can be subjected to increased buoyancy fluxes and to efficient mixing under winter atmospheric conditions.

Feliks (1991) incorporated stability dependent mixing, the effects of coasts and the recurrent forcing by winter storms into a two-dimensional model of the Levantine Basin, and was able to generate intermediate depth mixing and LIW formation in the entire region, with increased depth and uniformity along the coast.

It seems that either of the local production hypotheses in the above models are consistent with the observations. However, three-dimensional and isopycnal processes can exist at the same time. Packets of anomalous saline water have consistently been found on the periphery of the Rhodes Gyre (e.g. Özsoy *et al.*, 1989). Features similar to those in Fig. 15(f) were common during March 1989, and interleaving of waters with different properties were evident in many regions.

6.3. *Intermediate and deep convection during the winter of* 1991–1992

A set of unique observations in March 1992 (Sur *et al.*, 1992) have recently indicated intense mixing in the entire northern Levantine Basin, leading to simultaneous formation of LIW and Deep Water (DW), observed for the first time in the region. At the center of the Rhodes Gyre [Fig. 17(a)], uniform Deep Water properties ($\theta \simeq 13.7$, $S \simeq 38.8$) extended to depths of ≥1000 m. In the adjoining waters [Fig. 17(b)], a deep mixing layer (300–700 m) with uniform LIW properties ($\theta \simeq 15.2$–15.5, $S \simeq 39.1$–39.2) was found. The only previous occurrence of DW formation in the region was observed in 1987 by Gertman *et al.* (1990), in which case the uniform values observed at the center of the Rhodes Gyre ($\theta \simeq 14.0$, $S \simeq 38.9$) extended to depths of 500–600 m. Our observations indicate a recurrence with deeper, more efficient mixing 5 years later.

6.4. *Potential temperature–salinity relationships*

The water mass and mixing characteristics can be traced through the θ–S relationships (Figs 18–20), grouped together according to periods of apparent similarities. The first period [Fig. 18(a)–(e)] is from October 1985 to June 1987. Similar features are observed in September 1987, but this data set is excluded due to salinity drifts in the R.V. *Bilim* data. Figure 18(a) and (b), covering the entire Basin, is biased by an abundance of AW in the southern Levantine, relative to the other data sets covering only the north. A similar bias is also present between cruises of different areal coverage.

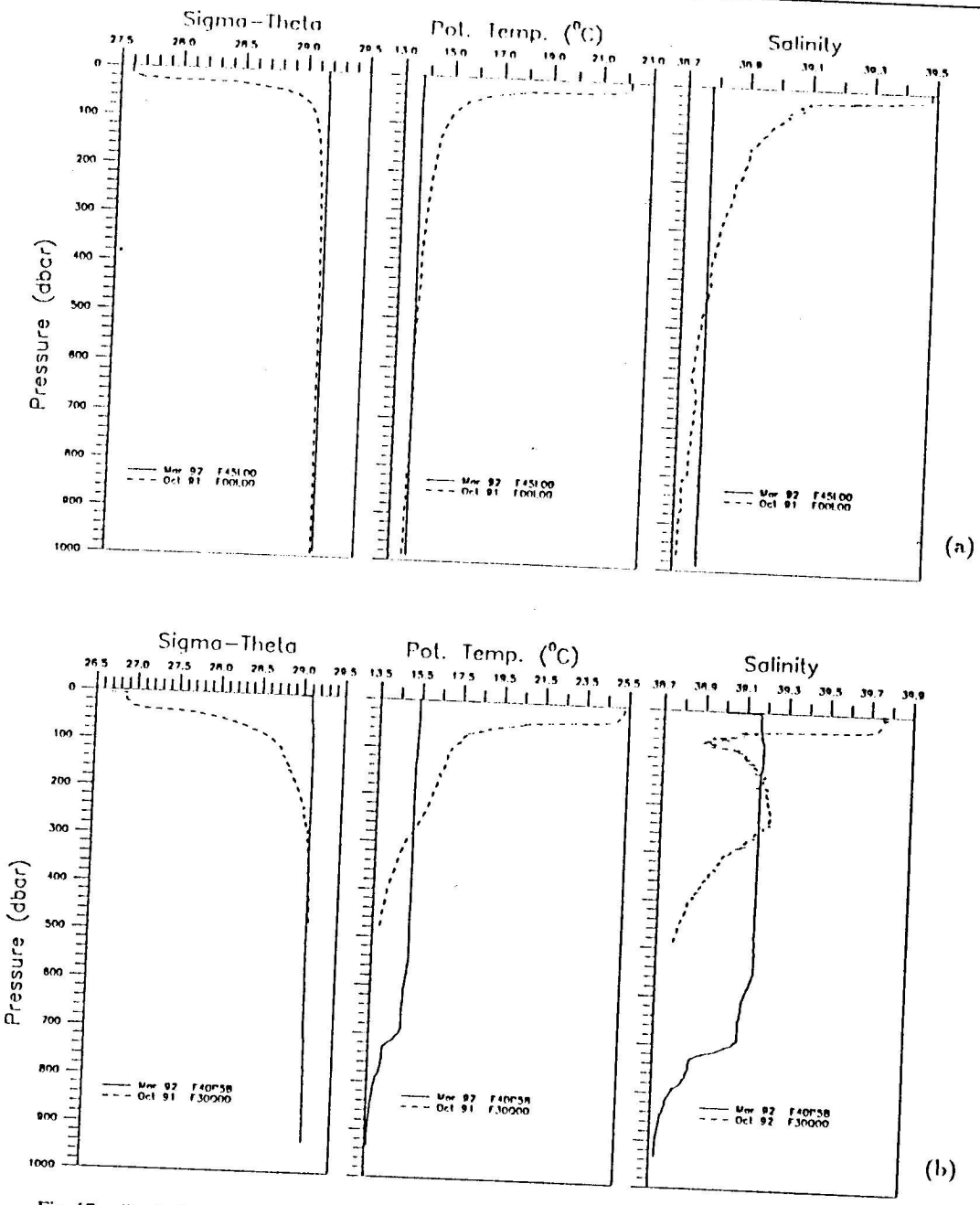

Fig. 17. Typical profiles of density (σ_θ), potential temperature (θ) and salinity (S) during October 1991 (dashed lines) and March 1992 (solid lines) observations: (a) within the Rhodes Gyre deep convection region; (b) in the intermediate depth convection region excluding the Rhodes Gyre (after Sur *et al.*, 1993).

In Fig. 18(a)–(e) the LIW is consistently detected in the form of a "spur" in the θ–S diagram, i.e. the collection of data points with $S \geq 39.1$, $\theta \simeq 16.1$ and $\sigma_\theta \simeq 28.9$. The data points represented by this particular shape correspond to LIW stored in the coherent anticyclonic eddies, mainly the Antalya (Özsoy *et al.*, 1989) and the Shikmona (Brenner *et al.*, 1991) eddies. Brenner *et al.* (1991) refer to this feature as a thermostad, i.e. the constant temperature and maximum salinities in the warm core eddy. It is important that the "spur" occurs predominantly during this period, most probably corresponding to LIW formed prior to our observations and maintained afterwards. For example, in March–April 1986 and February 1987 [Fig. 18(b) and (d)] the newly formed high salinity waters from the surface to intermediate depths do not appear to exceed the salinity values of the "spur". In June 1987 [Fig. 18(c)] the data points yielding the spur are from the Shikmona Gyre and not from Antalya eddy, which was shown to be modified in this period (Section 6.1).

The second group of θ–S diagrams [Fig. 19(a)–(c)] is for the 1988–1989 period, when important changes were detected in the circulation. In July–August and October 1988 [Fig. 19(a) and (b)], we observe that the earlier "spur" of the LIW has disappeared, probably as a result of mixing or leakage out of the region. The maximum salinity of the intermediate waters during these two cruises is ~39.0. There is also a reduced influence of AW, especially in the northern Levantine Basin. In March 1989 [Fig. 19(c)], the freshly formed LIW with ~39.2 salinity dominates the entire region.

Limited northern Levantine data obtained in August 1989, October 1989 and March 1990 display similar characteristics to the preceding period, with maximum salinities of ~39.1–39.2.

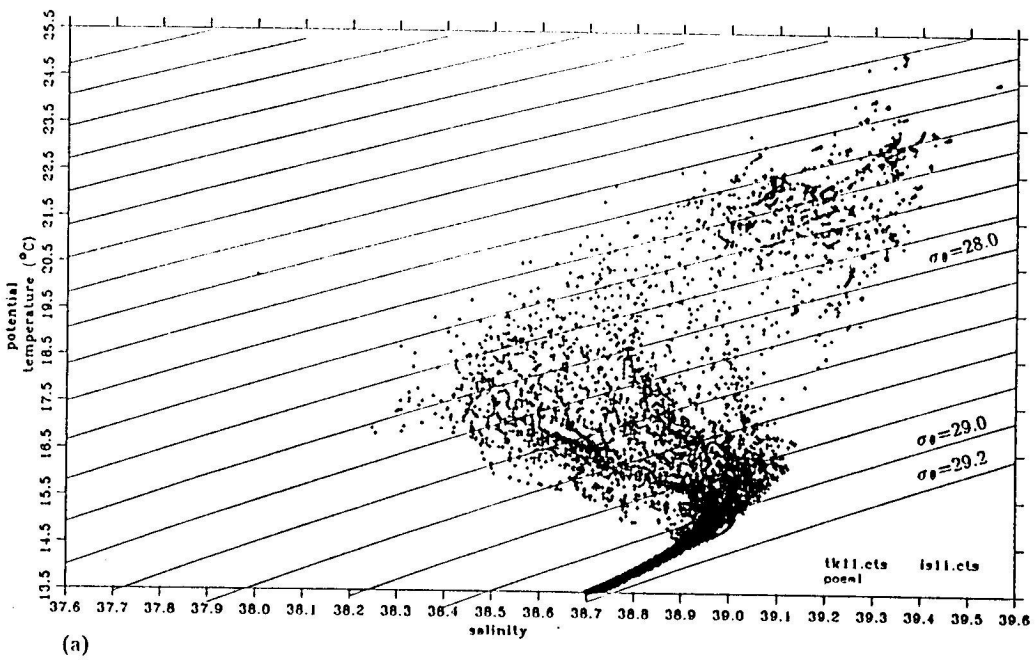

(a)

Fig. 18. Potential temperature vs salinity for (a) October–November 1985, (b) March–April 1986, (c) June 1986, (d) February 1987, (e) June 1987. (*Continued.*)

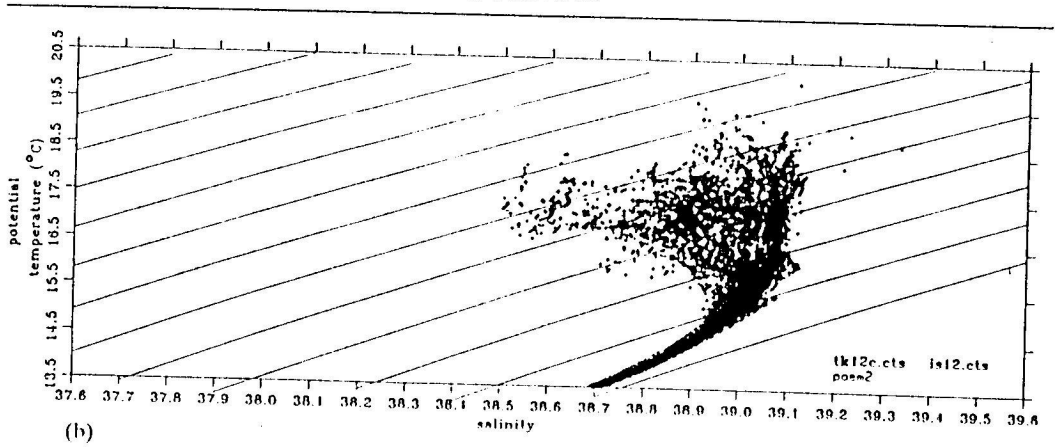

(b)

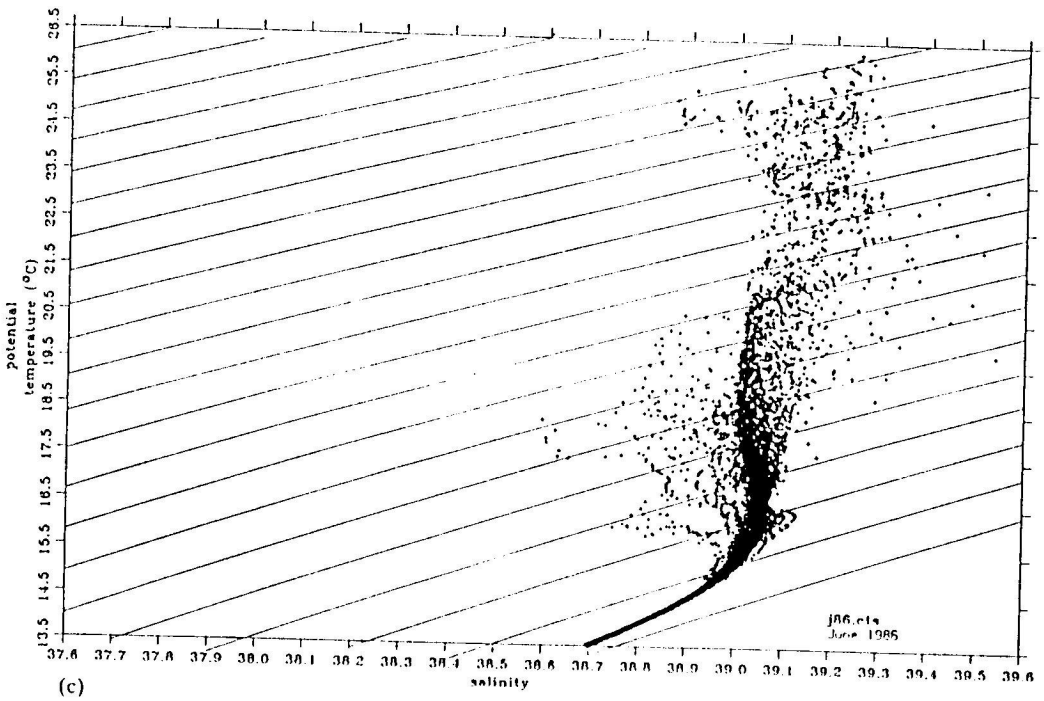

(c)

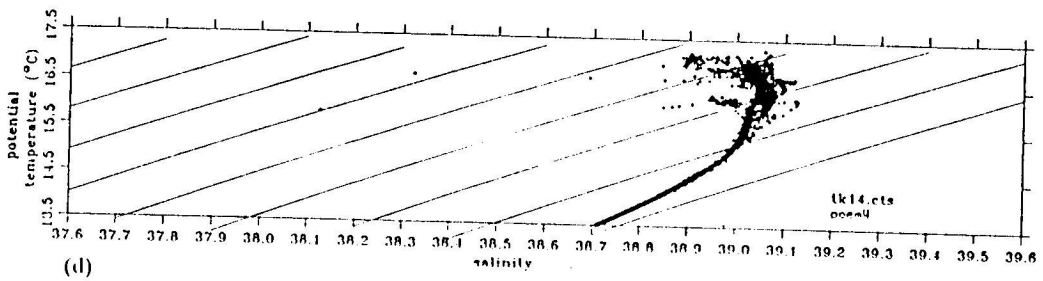

(d)

Fig. 18. (*Continued.*)

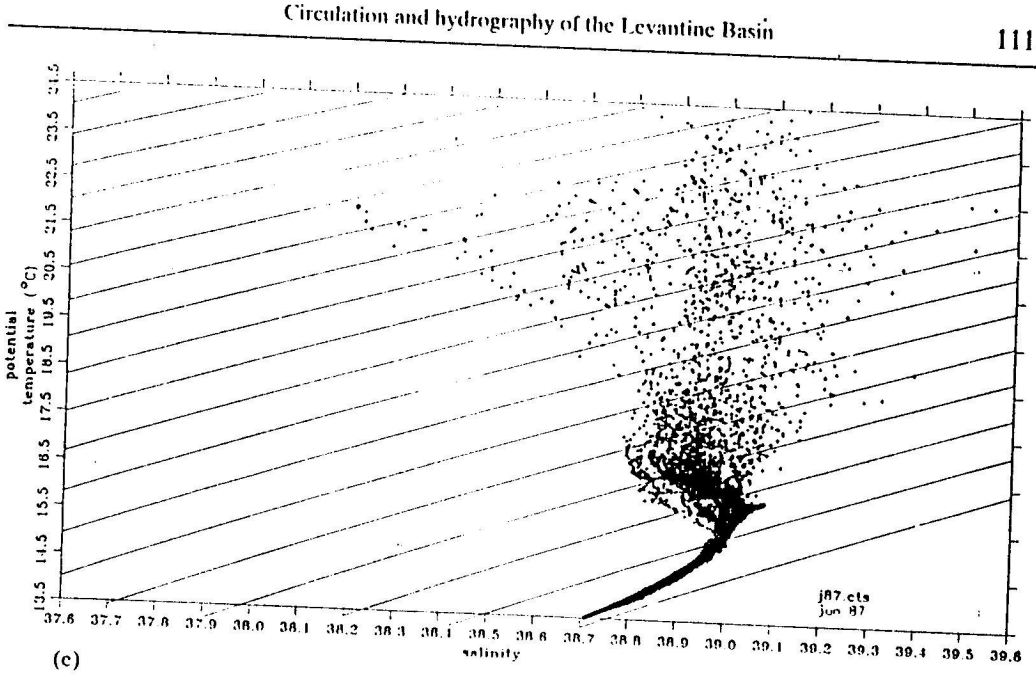

Fig. 18. (*Continued.*)

In the third period, August 1990, November 1990 and March 1991 [Fig. 20(a)–(c)], surface waters acquire high salinity values of ≈39.6, and initially the LIW has a salinity of ~39.2. In March 1991 the LIW salinities increase to ≥39.3. Increased surface fluxes may have caused the high surface salinity during the summer of 1990, which seems to have a bearing on the formation of high salinity LIW in March 1991.

Long term influences are evident in the formation and maintenance of LIW. The LIW is trapped in the cores of anticyclonic eddies in the first period, disappears later in response to the mixing and circulation changes in 1987. LIW with increasingly higher salinities is observed in the winter periods of the following years.

7. SUMMARY AND CONCLUSIONS

The Levantine Basin circulation consists of sub-basin-scale gyres driven by wind and thermohaline forcing, jets feeding the gyres, and a number of embedded coherent eddies. Although several scales are superimposed, stability and a high level of organisation are evident characteristics of the motions. The mesoscale signal is always present, but it does not seem to lead to rapid changes in the structure of the larger scale motions. Some circulations are persistent throughout the observation period (e.g. the Rhodes Gyre, the Shikmona eddy); others survive through extended periods (several months to a year, e.g. the Antalya and Crete eddies, the Asia Minor current). It is implicit in the observations that non-linear dynamics, confinement by the basin geometry, and bottom topography could play important roles in the Levantine Basin circulation. We find some coherent eddies locked into preferred positions and others co-evolving with the basin circulation.

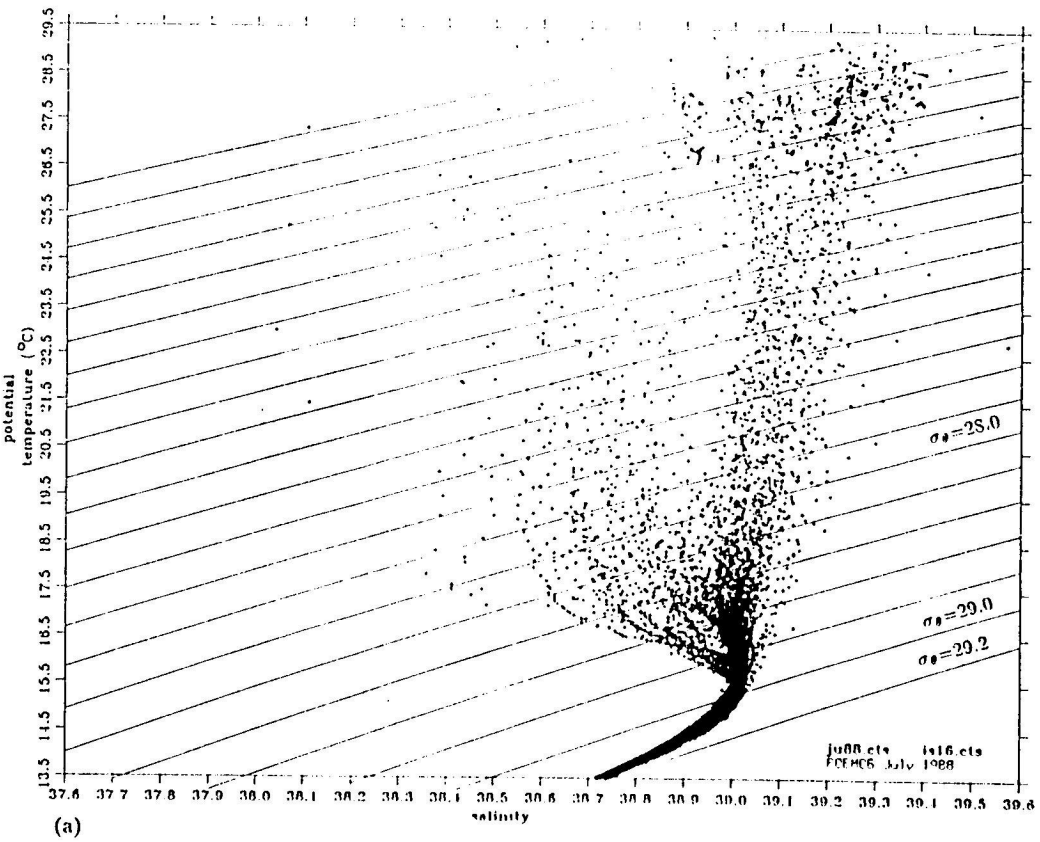

(a)

Fig. 19. Potential temperature vs salinity for (a) July–August 1988, (b) October 1988, (c) March 1989.

The circulation features appear closely related to the topography of the Rhodes Basin, the Anaximander Seamounts, the Mid-Mediterranean Ridge, the Eratosthenes Seamount, the depth transitions at Lattakia and Cilicia Basins, and the presence of the island of Cyprus.

The recurrence of the long-lived coherent features, such as the Antalya, Crete and Mersa Matruh eddies, and vacillations of the persistent Shikmona eddy are reminiscent of the emergence of coherent eddies in geophysical turbulence (McWILLIAMS, 1984). Combined effects of the planetary vorticity gradient and confinement by boundaries also can lead to coherent structures in the circulation (LARICHEV, 1989).

Model studies are expected to yield a better understanding of the underlying dynamics, although further progress is needed to resolve the above scientific questions. While the large scale circulations such as the Rhodes Gyre emerge (albeit displaced from realistic positions) in model simulations initialized with climatological data and forced by wind stress and buoyancy boundary conditions (e.g. PINARDI and NAVARRA, 1991; MALANOTTE-RIZZOLI and BERGAMASCO, 1989, 1991), relatively little success is obtained in generating coherent features such as the Shikmona, Antalya or Crete eddies, or the intense mid-basin

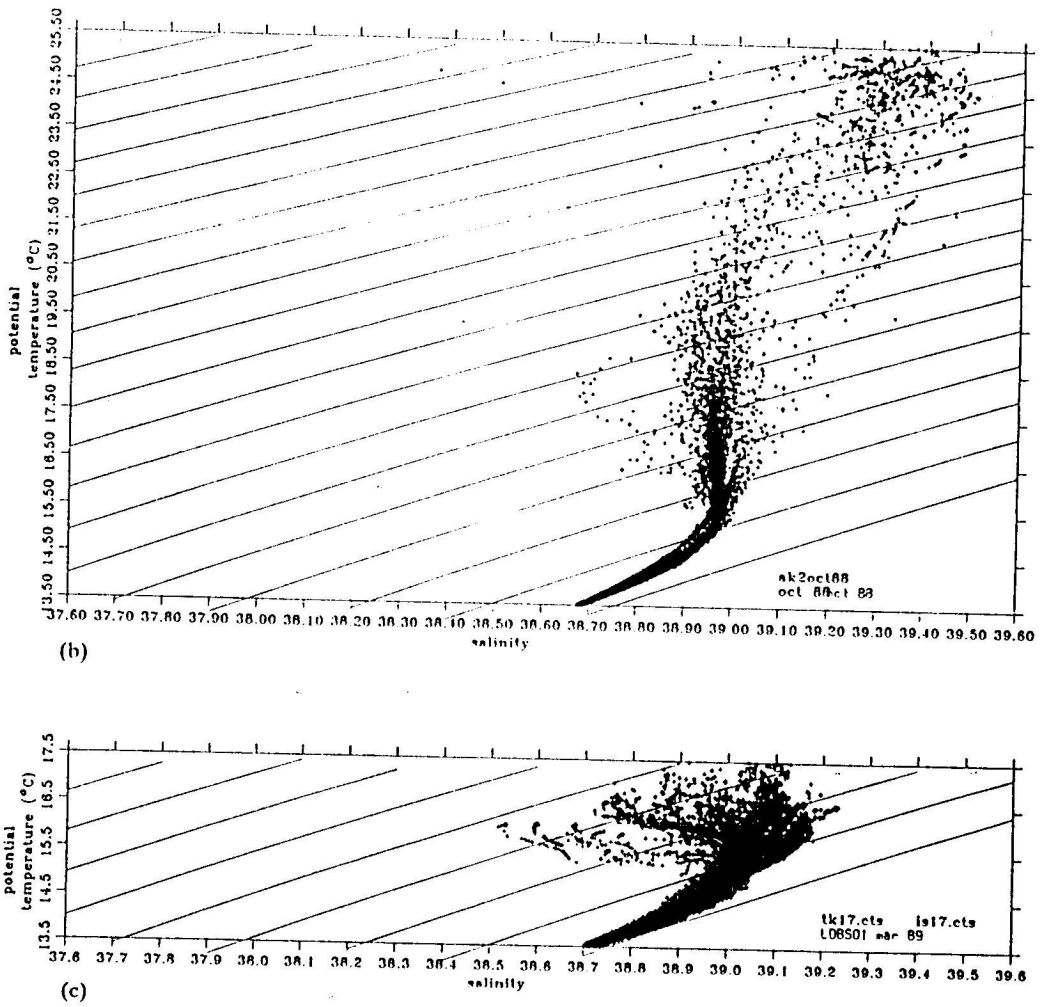

Fig. 19. (*Continued.*)

and coastal jets. On the other hand, long-lived coherent structures are supported by models once they are initialized with synoptic data containing such features (e.g. Robinson *et al.*, 1991b; Özsoy *et al.*, 1992; Milliff and Robinson, 1991).

Interannual variations and associated qualitative changes in the overall basin circulation, dispersion and mixing are evident in the observations, emphasizing the dominant role of climate interactions in the oceanography of the Levantine Basin. The particular setting of the Mediterranean Sea, as a temperate semi-enclosed sea located between land masses with great contrasts of climate, makes it predisposed to climatic interactions occurring via air–sea fluxes and modulated by the circulation, mixed-layer dynamics, and deep and intermediate depth convection. Impacts on biological components (including human concerns such as productivity, drought, etc.) in this environment deserve further study from a global change perspective.

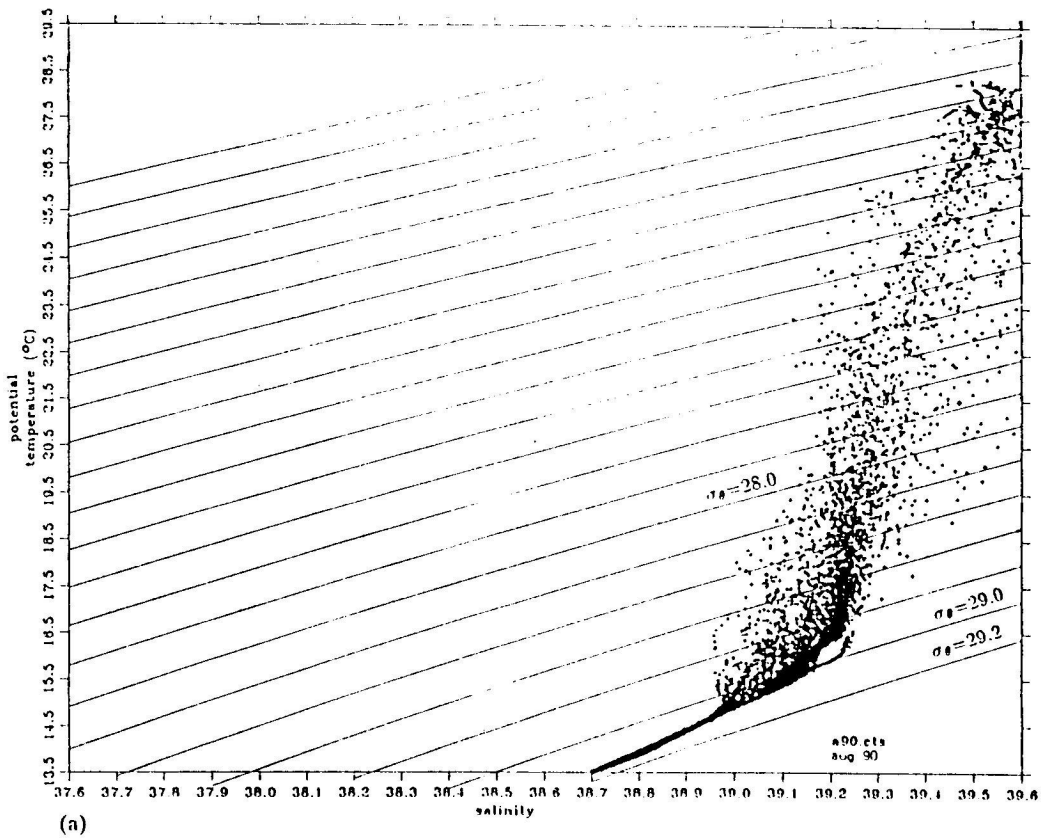

(a)

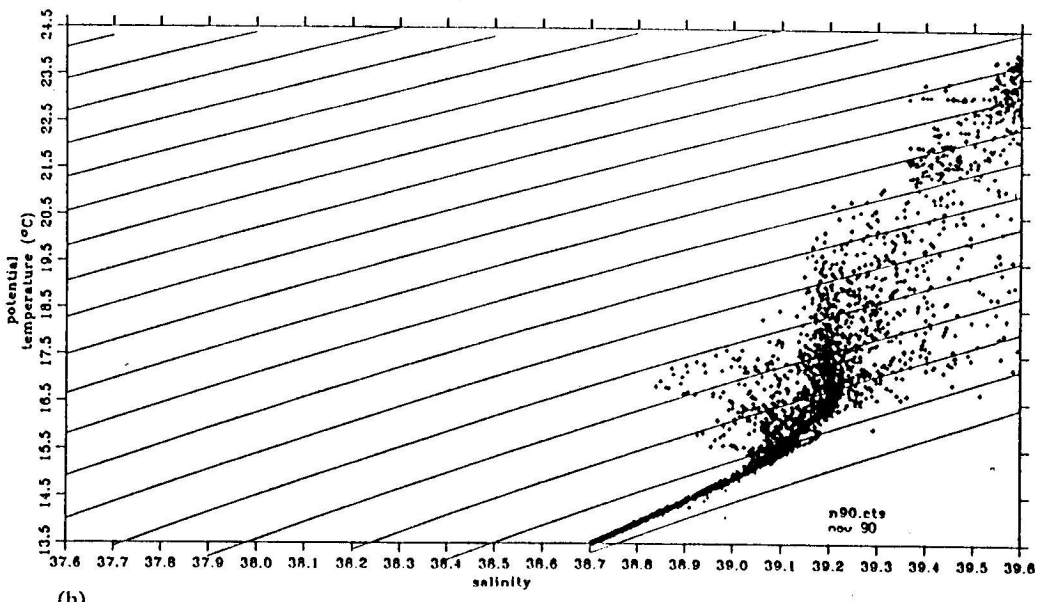

(b)

Fig. 20. (a) and (b).

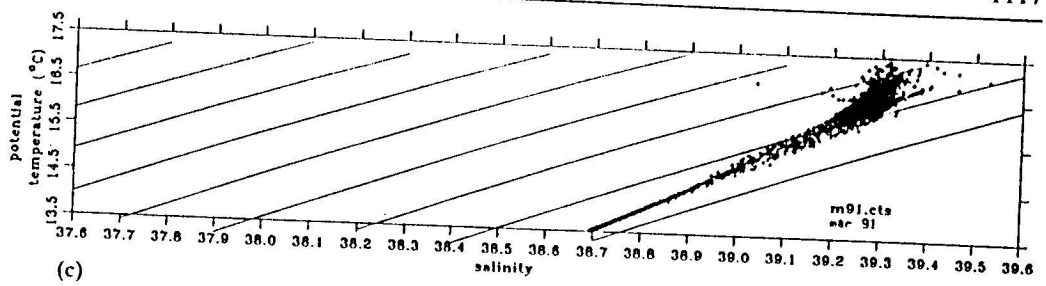

(c)

Fig. 20. Potential temperature vs salinity for (a) August 1990, (b) November 1990, (c) March 1991.

Acknowledgements—The oceanographic surveys of the R.V. *Bilim* were supported by the Turkish Scientific and Technical Research Council (TÜBITAK) under the National Oceanography Program. We thank several other members of the IMS-METU and the IOLR as well as the captains and crew of the R.V. *Bilim* and R.V. *Shikmona* for their hard work and contributions.

REFERENCES

Anati D. A. (1984) A dome of cold water in the Levantine Basin. *Deep-Sea Research*, **31**, 1251–1257.

Bergamasco A., P. Malanotte-Rizzoli, W. C. Thacker and R. B. Long (1993) The Seasonal Steady Circulation of the Eastern Mediterranean determined with the adjoint method. *Deep-Sea Research II*, **40**, 1269–1298.

Brenner S. (1989) Structure and evolution of warm core eddies in the Eastern Mediterranean Levantine Basin. *Journal of Geophysical Research*, **94**, 12593–12602.

Brenner S., Z. Rozentraub, J. Bishop and M. Krom (1991) The mixed layer/thermocline cycle of a persistent warm core eddy in the Eastern Mediterranean. *Dynamics of the Atmosphere and Oceans*, **15**, 455–476.

Brenner S. (1993) Long Term Evolution and Dynamics of a Persistent Warm Core Eddy in the Eastern Mediterranean Sea. *Deep-Sea Research II*, **40**, 1193–1206.

Brody L. R. and M. J. R. Nestor (1980) *Regional Forecasting Aids for the Mediterranean Basin, Handbook for Forecasters in the Mediterranean, Part* 2. Naval Environmental Prediction Research Facility, Monterey, California, Technical Report TR 80-10, 178 pp.

Bruce J. G. and H. Charnock (1965) Studies of winter sinking of cold water in the Aegean Sea, *Rapp. Comm. Int. Mer. Medit.*, **18**, 773–778.

Dewar W. K. (1986) Mixed layers in Gulf Stream rings. *Dynamics of the Atmosphere and Oceans*, **10**, 1–29.

Engel I. (1967) Currents in the Eastern Mediterranean. *International Hydrographic Review*, **44**, 23–40.

Feliks Y. (1991) Downwelling along the Northern Coast of the Eastern Mediterranean. *Journal of Physical Oceanography*, **21**, 511–526.

Garzoli S. and C. Maillard (1979) Winter circulation in the Sicily and Sardinia Straits region. *Deep-Sea Research*, **26A**, 933–954.

Georgopoulos D. A., D. A. Theocharis and G. Zodiatis (1989) Intermediate Water Formation in the Cretan Sea (South Aegean Sea), *Oceanologica Acta*, **12**, 353–359.

Gertman I. F., I. M. Ovchinnikov and Y. I. Popov (1990) Deep convection in the Levantine Sea. *Rapp. Comm. Mer Medit.*, **32**, 172.

Hecht A., N. Pinardi and A. Robinson (1988) Currents, water masses, eddies and jets in the Mediterranean Levantine Basin. *Journal of Physical Oceanography*, **18**, 1320–1353.

Lacombe H. (1975) Apercus sur l'apport a l'oceanographie physique des recherches recentes en Mediterrance. *Newslett. Coop. Invest. Medit.*, Special Issue, No. 7, 25 pp.

Larichev V. D. (1989) Differential Rotation (Beta-effect) as an Organizing Factor in Mesoscale Dynamics. In: *Mesoscale/synoptic coherent structures in geophysical turbulence*, J. C. J. Nihoul and B. M. Jamart, editors, Elsevier, pp. 41–49.

La Violette P. E. (1992) The Definition of Oceanographic Features in the Mediterranean Sea using Satellite Visible and Infrared Imagery. In: *Winds and currents of the Mediterranean Basin, Volume* II (proceedings of a NATO ASI at Santa Teresa, La Spezia, Italy, 1983) H. Charnock, editor, Reports in Meteorology and Oceanography, The Division of Applied Sciences, Harvard University, **40** and **41**, 175–216.

Malanotte-Rizzoli P. and A. R. Robinson (1988) POEM: Physical Oceanography of the Eastern Mediterranean. *EOS*, The Oceanography Report, **69**(15).

Malanotte-Rizzoli P. and A. Hecht (1988) Large-scale properties of the Eastern Mediterranean: a review. *Oceanologica Acta*, **11**, 323–335.

Malanotte-Rizzoli P. and A. Bergamasco (1989) The general circulation of the Eastern Mediterranean, Part I: The barotropic, wind-driven circulation. *Oceanologica Acta*, **12**, 335–351.

Malanotte-Rizzoli P. and A. Bergamasco (1991) The wind and thermally driven circulation of the Eastern Mediterranean Sea. Part II: The Baroclinic Case. *Dynamics of the Atmosphere and Oceans*, **15**, 355–419.

Manzella G. M. R., G. P. Gasparini and M. Astraldi (1988) Water exchange between the Eastern and Western Mediterranean through the Strait of Sicily. *Deep-Sea Research*, **35**, 1021–1035.

May P. W. (1982) *Climatological Flux Estimates of the Mediterranean Sea. Part I: Winds and Wind Stresses*. Report 54, NORDA, NSTL Station, 56 pp.

McClain C. R., G. Fu, M. Darzi and J. K. Firestone (1992) *PC-SEAPAK User's Guide, Version* 4.0. NASA Technical Memorandum 104557, NASA Goddard Space Flight Center, Greenbelt, MD.

McWilliams J. (1984) The emergence of isolated coherent vortices in turbulent flow. *Journal of Fluid Mechanics*, **146**, 21–43.

Middelandse Zee (1957) *Oceanographic and meteorological data*, Nederlands Meteorologisch Institut, 91 pp.

Milliff R. F. and A. R. Robinson (1992) Structure and dynamics of the Rhodes gyre system and dynamical interpolation for estimates of the mesoscale variability. *Journal of Physical Oceanography*, **22**, 317–337.

Morcos S. A. (1972) Sources of Mediterranean Intermediate Water in the Levantine Sea. In: *Studies in Physical Oceanography: a Tribute to G. Wüst on his 80th Birthday*, A. L. Gordon, editor, Gordon and Breach, New York, pp. 185–206.

Nielsen J. N. (1912) Hydrography of the Mediterranean and adjacent waters. In: *Report on the Danish Oceanographic Expedition 1908–1910 to the Mediterranean and Adjacent Waters*, **1**, 72–191. (Copenhagen).

Oren O. H. (1970) *Seasonal changes in the physical and chemical characteristics and the production in the low trophic level of the Mediterranean Waters off Israel*, Sea Fisheries Research Station, Haifa, Israel, Special Publication, 238 pp.

Ovchinnikov I. M. (1966) Circulation in the surface and intermediate layers of the Mediterranean. *Oceanology*, **6**, 143–148.

Ovchinnikov I. M., A. Plakhin, L. V. Moskalenko, K. V. Neglyad, A. S. Osadchiy, A. F. Fedoseyev, V. G. Krivoscheya and K. V. Voytova (1976) *Hydrology of the Mediterranean Sea*, Gidrometeoizdat, Leningrad, 375 pp.

Ovchinnikov I. M. (1984a) *Formation of Intermediate (Levantine) Waters in the Mediterranean Sea*, Academy of Sciences of the USSR, Doklady, Earth Science Sections, **270**, 214–217.

Ovchinnikov I. M. (1984b) The Formation of Intermediate Water in the Mediterranean. *Oceanology*, **24**, 168–173.

Ovchinnikov I. M. and A. Plakhin (1984) The Formation of Intermediate Waters of the Mediterranean Sea in the Rhodes Cyclonic Gyre. *Oceanology*, **24**, 317–319.

Özsoy E. (1981) *On the atmospheric factors affecting the Levantine Sea*. European Centre for Medium Range Weather Forecasts, Reading, U.K., Technical Report 25, 29 pp.

Özsoy E., C. Saydam, I. Salihoğlu and Ü. Ünlüata (1986) Sea surface expression of meso-scale eddies in the Northeastern Mediterranean—November 1985, Unesco/IOC First POEM Scientific Workshop, Erdemli, Turkey, 16–20 June 1986. In: *Physical oceanography of the Eastern Mediterranean (POEM): Initial Results*, Unesco Reports in Marine Science, **44**, 92 pp.

Özsoy E., A. Hecht and Ü. Ünlüata (1989) Circulation and Hydrography of the Levantine Basin. Results of POEM Coordinated Experiments 1985–1986. *Progress in Oceanography*, **22**, 125–170.

Özsoy E., C. Lozano, R. Milliff and A. R. Robinson (1990) *Quasigeostrophic Model Development for Multiply Connected Domains and Applications to the Levantine Basin Circulation*. Fourth POEM Scientific Workshop, Venice, Italy, 27 August–1 September, 1990.

Özsoy E., A. Hecht, Ü. Ünlüata, S. Brenner, T. Oğuz, J. Bishop, M. A. Latif and Z. Rozentraub (1991) A review of the Levantine Basin Circulation and its variability during 1985–1988. *Dynamics of the Atmosphere and Oceans*, **15**, 421–456.

Özsoy E. and Ü. Ünlüata (1991) Physical oceanography of the Eastern Mediterranean. In: *Proceedings of the 'Mediterranean Seas 2000' Symposium*, N. F. R. Della Croce, editor, Università di Genova, Istituto Scienza, Ambientali Marine, Santa Margherita, Ligure, Italy, pp. 207–253.

Özsoy E. and Ü. Ünlüata (1992) Dynamical aspects of the Cilician Basin, Northeastern Mediterranean. In: *Winds and currents of the Mediterranean Basin, Volume* II (proceedings of a NATO ASI at Santa Teresa, La Spezia, Italy, 1983), H. Charnock, editor, Reports in Meteorology and Oceanography, The Division of Applied Sciences, Harvard University, **40** and **41**, pp. 1–34.

Özsoy E., C. Lozano and A. R. Robinson (1992) A Baroclinic Quasigeostrophic Model for Closed Basins or Semi-Enclosed Seas with Islands. *Mathematics and Computers in Simulations*, **34**, 51–79.

Pavia, E. G. and B. Cushman-Roisin (1990) Merging of frontal eddies. *Journal of Physical Oceanography*, **20**, 1886–1906.

Philippe M. and L. Harang (1982) Surface temperature fronts in the Mediterranean Sea from infrared satellite imagery. In: *Hydrodynamics of Semi-Enclosed Seas*, J. C. J. Nihoul, editor, Elsevier, pp. 91–128.

Pinardi N. (1988) *Report of the POEM mapping group meeting—POEM-V-87 General circulation survey data set preparation*, Modena, Italy, 7–18 March 1988. IMGA-CNR Technical Report 1-88.

Pinardi N. and A. Navarra (1989) *A brief review of global Mediterranean wind-driven general circulation experiments*. Second POEM Scientific Workshop, OGS, Trieste, Italy, 31 May–4 June, 1988, POEM Scientific Reports No. 3, 162 pp.

Pinardi N. and A. Navarra (1992) Baroclinic Wind Adjustment Processes in the Mediterranean Sea. *Deep-Sea Research II*, **40**, 1299–1326.

The POEM Group [A. R. Robinson, P. Malanotte-Rizzoli, A. Hecht, A. Michelato, W. Roether, A. Theocharis, Ü. Ünlüata, N. Pinardi, A. Artegiani, J. Bishop, S. Brenner, S. Christianidis, M. Gacic, D. Georgopoulos, M. Golnaraghi, M. Hausmann, H.-G. Junghaus, A. Lascaratos, M. A. Latif, W. G. Leslie, T. Oğuz, E. Özsoy, E. Papageorgiou, E. Paschini, Z. Rosentroub, E. Sansone, P. Scarazzato, R. Schlitzer, G.-C. Spezie, G. Zodiatis, L. Athanassiadou, M. Gerges and M. Osman] (1992) General circulation of the Eastern Mediterranean. *Earth Science Reviews*, **32**, 285–309.

Reiter E. R. (1975) *Handbook for forecasters in the Mediterranean; weather phenomena of the Mediterranean Basin; Part* 1: General Description of the Meteorological Processes, Environmental Prediction Research Facility, Naval Postgraduate School, Monterey, California, Technical Paper No. 5-75, 344 pp.

Robinson A. R., A. Hecht, N. Pinardi, J. Bishop, Z. Leslie, A. J. Rosentraub, A. J. Mariano and S. Brenner (1987) Small synoptic/mesoscale eddies and energetic variability of the Eastern Levantine Basin. *Nature*, **327**, 131–134.

Robinson A. R., M. Golnaraghi, W. G. Leslie, A. Artegiani, A. Hecht, A. Michelato, E. Sansone, A. Theocharis and Ü. Ünlüata (1991a) The Eastern Mediterranean general circulation: Features, structure and variability. *Dynamics of the Atmosphere and Oceans*, **15**, 215–240.

Robinson A. R., M. Golnaraghi, C. J. Lozano, R. Milliff and E. Özsoy (1991b) *Data assimilation in quasigeostrophic model with arbitrary coasts and islands*, 23rd International Liege Colloquium on Ocean Hydrodynamics, Modelling the Interaction of the Deep Ocean and the Shelf and Coastal Seas, Liege, 6–10 May 1991.

Schmitt R. W. and D. B. Olson (1985) Wintertime Convection in Warm Core Rings: Thermocline Ventilation and the Formation of Mesoscale Lenses. *Journal of Geophysical Research*, **90**, 8823–8837.

Sur H. I., E. Özsoy and Ü. Ünlüata (1992) Simultaneous deep and intermediate depth convection in the Northern Levantine Sea, winter 1992. *Oceanologica Acta*, in press.

Tziperman E. and P. Malanotte-Rizzoli (1991) The Climatological Seasonal Circulation of the Mediterranean Sea. *Journal of Marine Research*, **49**, 411–434.

UNESCO (1984) *Physical Oceanography of the Eastern Mediterranean: An Overview and Research Plan*, UNESCO, Reports in Marine Science, Paris, Report No. 30, 16 pp.

UNESCO (1985) *Physical Oceanography of the Eastern Mediterranean (POEM): A Research Programme*, UNESCO, Reports in Marine Science, Paris, Report No. 35, 67 pp.

UNESCO (1987) Physical Oceanography of the Eastern Mediterranean (POEM) Initial results, UNESCO/IOC, Reports in Marine Science, Turkey, 16–20 June 1986, UNESCO, Paris, Report No. 44, 92 pp.

Wüst G. (1961) On the Vertical Circulation of the Mediterranean Sea. *Journal of Geophysical Research*, **66**, 3261–3292.